# SEISMIC PERFORMANCE OF IRREGULAR RC FRAMES DESIGNED ACCORDING TO THE DDBD APPROACH

P. Giannakouras[1] and C. Zeris[2]

Direct Displacement Based Design; reinforced concrete; irregular frame; height irregularity; seismic design; ductility; nonlinear analysis

[1] Post Graduate Structural Engineer, National Technical University of Athens, Greece, p.giann17@gmail.com

[2] Corresponding Author: Associate Professor, Laboratory of Reinforced Concrete, School of Civil Engineering, National Technical University of Athens, Greece, zeris@central.ntua.gr

## ABSTRACT

The Direct Displacement-Based seismic Design (DDBD) method has been a major development in the context of Performance-Based seismic Design of reinforced concrete (RC) frames. The method has been positively received from the engineering community, while, at the same time, significant improvements have been proposed. Even though its field of application is constantly widening, no specific rules are generally provided for specific cases, such as RC frames with setback irregularity, under the claim that, in this case, no modifications in the basic approach are needed. The validity of this assumption is examined by assessing the DDBD provisions through design of such irregular RC structures and assessment of their seismic performance under non-linear static and dynamic analyses. Local ductility associated with global behavior is examined and incompatibilities in demands with the global design displacement are identified, where they occur. Guidelines are provided to ensure that rational performance results are obtained, when the DDBD method is applied.

## 1. Introduction and Statement of the Problem

Taking advantage of the post-elastic behavior of materials is critical in order to design both safe and economic structures against seismic excitations. To that end, a rational approach in earthquake engineering is Performance-Based Design (PBD), where performance levels are defined and a different damage level is prescribed for every performance level set (SEAOC 1995). The damage that a structure exhibits is directly related to the displacements that are predicted during the structure's response. Parallel to the evolution of conventional seismic design, still currently enforced to a PBD context, extensive efforts have recently been given towards formulating alternative seismic design methodologies that make use of the global structural displacement, instead of the acceleration response and the corresponding inertial force, as the controlled design parameter. One of the most promising methods is the Direct Displacement-Based Design (DDBD) approach, primarily developed by Priestley *et al.* (2007). Reliable guidelines for the implementation of this methodology for the seismic design of a wide range of structures were incorporated into DBD12, the Model Code for DDBD (Sullivan *et al.* 2012), while investigations are ongoing for improvement of the method, that will inevitably lead to further revisions of this code.

Significant efforts have been made towards the extension of the applicability of the DDBD approach to different structural building forms and structural materials other than reinforced concrete (RC) (Vidot-Vega and Kowalsky 2013), such as structural steel (Malekpour *et al.* 2013) and masonry (Paparo and Beyer 2015), while keeping its simplicity unaffected. The method has also found increasing applicability in the seismic design of bridges, due to the relatively simpler structural configuration of this type of structural system (Mergos 2013, Gkatzogias and Kappos 2015, Amiri et al. 2016) and innovative structural systems, such as base isolation (Cardone *et al.* 2010) and precast prestressed concrete (Yang and Lu 2017). Meanwhile, engineers are encouraged to implement state-of-the-art techniques in everyday practice, such as non-linear analyses, to verify the performance of the structure under consideration. Furthermore, explicit rules or modifications of the basic DDBD approach are not readily available for many commonly encountered structural irregularities such as vertical setback buildings, since, it is claimed, in this case the storey mass to stiffness ratio remains essentially constant. Vertical setbacks are often imposed by architectural considerations and significantly affect the seismic response, as post-earthquake field observations (Inel and Meral 2016) or different analytical studies of conventionally design irregular buildings have demonstrated (Zhou *et al.* 2015, Landi *et al.* 2014, Nezhad and Poursha 2015). However, irregular RC frames have received comparatively little attention within the context of the DDBD approach. Nievas and Sullivan (2015) modified the higher mode effects reduction factor $\omega_\theta$ for steel plane frames with setbacks. Varughese *et al.* (2012) focused on the base shear distribution in in-height stepped buildings, including torsional effects and, more recently, for the DDBD of soft open ground story buildings (Varughese *et al.* 2015). Other types of irregularities, such as out-of-plane-offsets in frames, have also been assessed in the recent literature (Muljati *et al.* 2015).

Currently, two methods of analysis have been proposed in DDBD for estimating the required flexural strength of plastic hinges (Priestley *et al.* 2007). According to the first method, conventional structural analysis is conducted, using modeling assumptions that conform to the design procedure approximations for an accurate estimation of members' stiffness. Alternatively, approximate calculations based on equilibrium considerations and appropriate assumptions can be employed, thus eliminating the need for member stiffness estimation. Even though the abundance of conventional analysis software renders the first method easier to apply, researchers prefer the second method. The inevitable approximate nature of the structural analysis process and the uncertainties associated suggest that simplified procedures such as the second method are attractive.

The scope of this work is to investigate the applicability of the DDBD conventional analysis approach on plane RC frames with height irregularity in the form of setbacks, with emphasis on the comparison of local demands that are imposed to the members under nonlinear static and dynamic analysis with the design assumed values. To that effect, Seven and Ten Storey RC frames with constant bay widths and setbacks and their regular counterparts, were designed according to the current DDBD approach (Sullivan *et al.* 2012). The influence of the design analysis method is examined, by comparing the final designs of the Seven Story frames, designed by the application of either of two conventional approaches, namely the direct approach and an iterative approach for establishing the design moment capacity. Furthermore, since unequal bay lengths may introduce unequal local demands at the beams (O'Reilly *et al.* 2017), a set of irregular Ten Storey frames with unequal bays is also examined.

Nonlinear static and dynamic time-history analyses are conducted and the results are compared with design predictions, while differences in the response of both the regular and the irregular frames and the influence of higher modes and second order (P-$\delta$) effects, are addressed. While the vast majority of DDBD research deals with the limitation of global storey drifts within the design adopted performance limit state related limits, special attention is paid in this work to the local ductility demands associated with the prescribed global deformation ductility and possible exceedances from design expected response are examined. The successful application of the DDBD method is judged by an integrated approach, where global displacement objectives and local ductility criteria are simultaneously met.

## 2. Brief Description of the DDBD Method

In order to evaluate the basic assumptions inherent in the basic DDBD procedure, a brief outline of the method is considered. The method is based on the substitution of the actual structure with an equivalent single-degree-of-freedom system (e-SDOF). The e-SDOF representation is characterized by the effective stiffness that corresponds to either the peak displacement response or the target displacement of the design performance level, instead of the initial elastic stiffness of the SDOF system. Using the design displacement profile of the actual structure, the equivalent properties of the e-SDOF, namely its design displacement $\Delta_d$, effective mass $m_e$ and effective height $H_e$ are derived, as weighted average values of the corresponding actual properties (Sullivan *et al.* 2012). The design of moment resisting frames is likely to be governed by code prescribed drift limitation rather than material strain limits, so their design displacement profile is based upon the determination of the maximum allowable global drift $\theta_c$ for the design limit state. For repairable damage, $\theta_c$ = 2.5% is assumed. Following the definition of $\theta_c$, Eq. (6.2) of Sullivan *et al* (2012) provides the limit state displacements at each storey, as a function of the global drift. These values correspond to the first inelastic mode of vibration. Since higher modes can increase the deformations, they are multiplied with a reduction factor $\omega_\theta$, which is provided by Fig 5.1 of Sullivan *et al* (2012) in order to obtain the design displacements.

It is evident that the dimensionless yield curvature of a cross-section remains comparatively invariant (Priestley *et al 2007*). As a result, an expression that provides the yield drift $\theta_y$ of a frame building with an enforced weak beam – strong column mechanism can be derived, leading to the evaluation of the yield displacement (see Eqs. C7.1 & 7.2 of Sullivan *et al* (2012)) and subsequently the design global displacement ductility $\mu$. The equivalent viscous damping (EVD) coefficient $\xi_{eq}$ of the e-SDOF is then calculated; EVD represents the combined elastic and hysteretic energy absorbed during the inelastic response that is prescribed by the aforementioned displacement ductility. Assuming an appropriate hysteretic rule for RC frames, such as the rule proposed by Takeda (1970), with parameters α and β equal to 0.3 and 0.6 respectively (Eq. (7.4) of

Sullivan *et al.* 2012), yields $\xi_{eq}$ from the design global ductility $\mu$.

After selecting an appropriate design displacement spectrum consistent with the seismic design intensity, the damped spectral ordinates are calculated using a damping reduction factor. A typical displacement spectrum comprises an approximately linear ascending branch followed by a constant displacement plateau at the spectrum corner point period and displacement $T_D$ and $\Delta_{D,\xi}$, with all the relevant design properties indexed *D*. The non-linearity at low periods, corresponding to the constant acceleration period range, can be safely disregarded. Currently, the appropriate damping reduction factor $R_\xi$ is given by Eq. (1.2) of Sullivan *et al.* (2012). It is noted, however, that the calculation of the inelastic displacement demand is subject to further development, such as adopting the findings of Pennucci *et al* (2011), also incorporated in Annex 2 of Sullivan *et al* (2012). If the design displacement does not exceed the damped spectrum corner displacement $\Delta_{D,\xi}$, as is common for RC frames in moderate to high seismicity, the effective period of the e-SDOF structure is obtained from Eqs. (1.1) and (5.6) of Sullivan *et al* (2012), thereby yielding the effective stiffness of the e-SDOF system $K_e$ (Eq. 5.4 of Sullivan *et al* 2012).

The influence of P-$\delta$ effects is directly incorporated into the DDBD design process by increasing the total base shear force $V_{base}$ by an additional force $V_{P-\Delta}$, if the stability coefficient of the e-SDOF structure namely $m_e g/K_e H_e$, exceeds 0.05. Furthermore the stability coefficient of each storey should not exceed 0.30, which would rarely be the case for RC frames. The total base shear force can be obtained from Eqs. (5.1) and (5.8) of Sullivan *et al* (2012). An upper bound is usually checked in order to correct for the response at extremely low periods of vibration, where the displacement spectral shape has been distorted. In order to evaluate the flexural strength of plastic hinges, the design base shear is distributed as equivalent lateral forces according to the distributions of the storey masses $m_i$, using Eqs. (8.1a)–(8.1b) (Sullivan *et al* 2012). Structural analysis of the model can now be performed, yielding the design internal forces. As noted above, two alternative methods have been proposed to perform analysis, both requiring the determination of the column base flexural strength by utilizing equilibrium considerations.

Upon completion of the analysis, bending moments at joint faces, shear and axial forces are readily available. Detailing of plastic hinges is performed by moment – curvature analyses of the sections where hinging is expected. Such analyses are conducted with material strain limits depending on the design limit state, using expected material strengths without reduction partial factors. On the other hand, strength for capacity protected actions (shear, flexure in locations where no plastic hinges are expected to form) is calculated with characteristic values of the material capacities, reduced by partial factors. The required dependable strength for these sections is derived from the value corresponding to the design lateral force distribution, amplified due to material overstrength and higher mode effects. The required column flexural and shear strengths, in particular, are obtained from Eqs. (9.2)-(9.5) of Sullivan *et al* (2012), respectively. If no further calculations are performed, a material overstrength factor $\varphi_o$ equal to 1.25 is assumed. The higher mode dynamic amplification factor $\omega_f$ is height dependent and is obtained from Fig (9.1) of Sullivan *et al* (2012), for plane frames.

Having outlined the basic DDBD method, it is noted that the local ductility demands are not explicitly defined in terms of plastic rotation or other, during the design process. No minimum curvature ductility is prescribed and, consequently, no confining reinforcement is dictated, as in current force based seismic design codes (EC8-1 2004). It is therefore assumed that the strain limits adopted during the section detailing would suffice in providing the necessary local ductility. To accommodate the needs of the present study, the design plastic rotation is defined for every plastic hinge by multiplying the design plastic curvature with the plastic hinge length, proposed by Priestley *et al.* (2007), as also outlined in the following section.

## 3. Description of the Frames and DDBD Design Procedure

The basic geometry of the Seven-Storey and Ten-Storey frames that are investigated herein is depicted in Figs.1a, 1b. The frames consist of three bays with constant bay length equal to 6m. Furthermore, for the Ten-Storey building, a set of frames with unequal bays (6m – 3m – 6m) is introduced, with different locations of the unequal bay within the setback. Storey height is retained constant in all the frames, and is equal to 3m at all levels. There is no setback at the perpendicular direction of irregular buildings, so no torsional response is anticipated. As a result, the seismic response can be decoupled and plane frame models describe adequately the behavior of the structures. Frame spacing at the perpendicular direction is equal to the bay length. Due to the monolithic nature of RC structures, seismic forces are resisted by every frame in the respective direction. As a result, two unique frames exist for each building with different seismic masses (inner and outer). A typical plan is illustrated in Fig.2, where the tributary areas that are used for the distribution of the slab loads to the beams are also depicted.

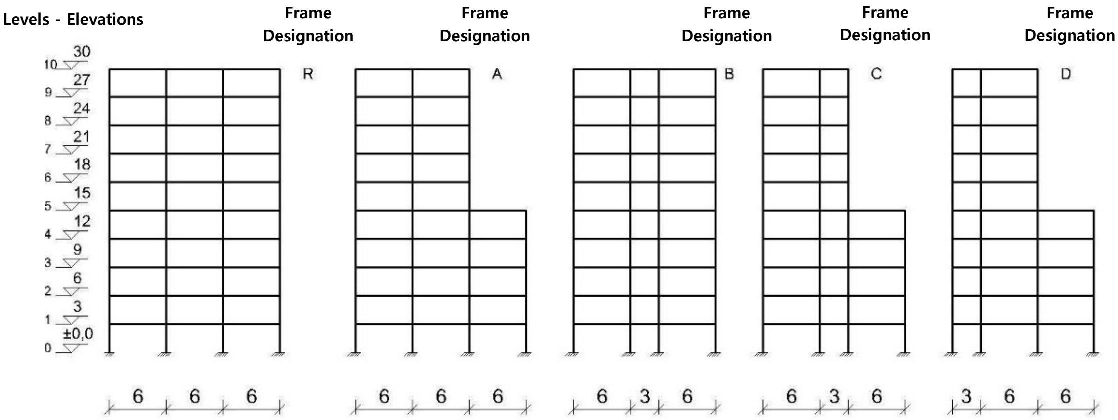


Fig. 1a Frame elevations of the Ten-Storey Frames

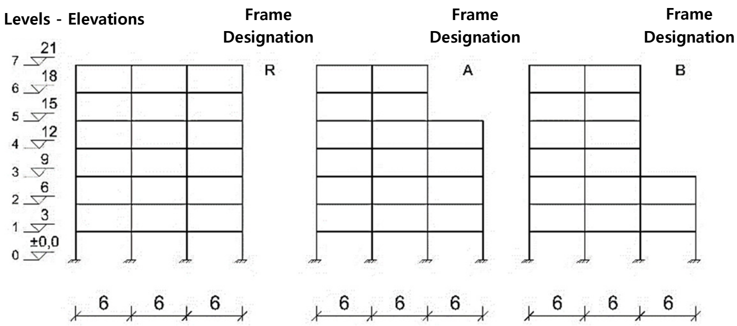


Fig. 1b Frame elevations of the Seven-Storey Frames

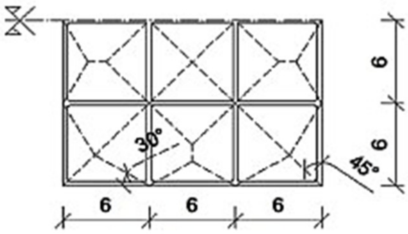


Fig. 2 Typical Plan View

The gravity loads were considered according to the seismic combination G+0.3Q (EC8-1 2004). Maximum factored gravity loads - combination 1.35G+1.50Q (EC8-1 2004) was also taken into account and governed the required flexural strength of the roof beams. The self weight was evaluated as 4.0 kN/m$^2$, assuming constant slab thickness equal to 0.16m and typical element cross-sections. Super-imposed dead load and live load were also accounted, with characteristic values equal to 1.5 kN/m$^2$ and 2.0 kN/m$^2$ respectively. Interior moveable masonry partitions were substituted by an equivalent uniformly distributed load equal to 1.0 kN/m$^2$. The perimeter infill is only applied to the outer frame beams as a line load with characteristic value 9.0 kN/m. It is suggested that the plastic hinges are designed for either the maximum factored gravity loads or the seismic loads only, while the axial force of column bases is derived only from the gravity loads. (Priestley *et al.* 2007).

Beam height governs the yielding of frames and has to be predefined in order to proceed with the calculations. For the frames considered, a beam height equal to 0.60m was selected. Columns are square and their size is defined with respect to the upper limits of the normalized axial force proposed by EC8 (2004). Column size is also reduced with height and is only needed when the calculation of moments at joint faces is performed. The seismic mass of stories without setback for outer and inner frames is equal to 65 tons and 87 tons, respectively while, for setback stories, it is reduced to 43 tons and 58 tons, respectively.

In Fig.3a and 3b, the design displacement profiles of the Seven-Storey and the Ten-Storey Frames (R or A) are given for the design assumed limit state of repairable damage ($\theta_c$ = 2.5%). For the evaluation of the design plastic rotations, frame members are considered as equivalent cantilevers and the design plastic curvature is calculated using the design drift above as input, following Priestley *et al.* (2007). It is assumed that each storey's beams are subject to plastic rotations stemming from the drift demand of the respective storey lower columns. For example, design plastic rotations of the 2$^{nd}$ storey beams are calculated using the drift demands of the second storey columns (Fig. 3c); it is, therefore, reasonably assumed that a storey's beams are subjected to the largest rotation induced to the joint by the columns. The equivalent cantilevers' length was taken as follows: for beams, it was assumed equal to the half of the clear span, neglecting for gravity loads, an approximation which is compatible with the DDBD approach. For ground floor columns, it was explicitly defined during the calculation of the required strength at the column bases. Other columns are capacity protected from inelastic action and, therefore, no design plastic rotation is defined.

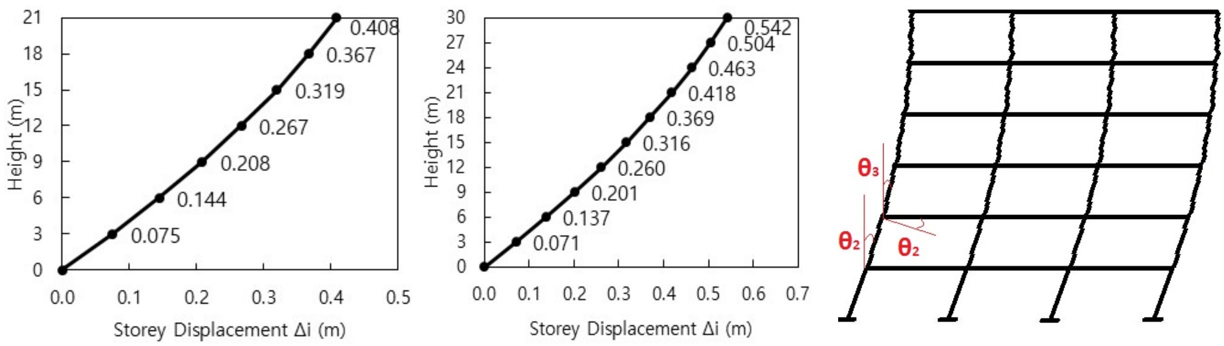


(a) (b) (c)

Fig. 3 Design Displacement Profiles of a) the Seven – Storey and b) the Ten – Storey Frames (R or A); and c) Evaluation of the typical 2$^{nd}$ storey beam plastic rotation.

It has been repeatedly reported that the current codified displacement spectra are incapable of reliably predicting the displacement demand in the medium and high period range (Akkar and Bommer (2007), Priestley *et al.* (2007), Cauzzi *et al.* (2008)). A finding that has been attested by the authors, since designing frames to DDBD using EC8 elastic displacement spectrum without any modifications led to unrealistic results. Therefore, seismological research has focused on the reliable estimation of appropriate spectral values in the long period range, to accompany the DDBD method. Priestley *et al.* (2007) propose Eqs. (1) – (2) for the corner period $T_D$ (transition period between constant spectral velocity and constant spectral displacement areas) and the peak displacement response $\delta_{max}$, respectively (Faccioli *et al.* 2004), also adopted herein. For design purposes, a typical seismic scenario of a moment magnitude $M_w$ = 7 earthquake at an epicentral distance $R$ = 10 km on firm ground ($C_s$ = 1) was assumed, yielding the design displacement spectrum used in the present study with $T_D$ = 4.25s and $\Delta_{D,5\%}$ = 0.631m (Eqs. (1), (2)):

$$T_D = 1 + 2.5(M_w - 5.7) \tag{1}$$

$$\delta_{max} = \Delta_{D,5\%} = C_s \cdot \frac{10^{M_w - 3.2}}{R} \tag{2}$$

The e-SDOF properties that result from the application of the DDBD procedure described in Section (2) are summarized in Table 1. For simplicity, only the results of the outer frames (types A and R) are provided, with the response parameters of the other cases being similar.

Table 1. Properties of the case structures' e-SDOF systems.

| Frames | Seven-storey | | Ten storey | |
|---|---|---|---|---|
| | A | R | A | R |
| Design Displacement $\Delta_d$ (m) | 0.290 | 0.304 | 0.400 | 0.423 |
| Yield Displacement $\Delta_y$ (m) | 0.189 | 0.201 | 0.264 | 0.281 |
| Ductility $\mu$ | 1.53 | 1.52 | 1.52 | 1.50 |
| % EVD $\xi_{eq}$ | 11.24 | 11.11 | 11.13 | 11.03 |
| Damped Corner Displacement $\Delta_{D,\xi}$ (m) | 0.459 | 0.461 | 0.461 | 0.462 |
| Effective Fundamental Period $T_e$ (s) | 2.68 | 2.80 | 3.69 | 3.89 |
| Effective Mass $m_e$ (tons) | 342.5 | 382.2 | 432.7 | 536.2 |
| % Effective to Total Seismic Mass | 83.3 | 84.0 | 80.1 | 82.5 |
| Effective Height $H_e$ (m) | 13.75 | 14.61 | 19.18 | 20.46 |
| % Effective to Total Building Height | 65.5 | 69.6 | 63.9 | 68.2 |
| Base Shear $V_{base}$ (kN) | 543.6 | 583.7 | 545.9 | 646.8 |
| % Base Shear to Total Seismic Weight $R_V$ | 13.5 | 13.1 | 10.3 | 10.1 |
| % e-SDOF Stability Coefficient $\theta_{P-\Delta}$ | 14.4 | 14.8 | 17.7 | 18.4 |
| Additional Base Shear $V_{P-\Delta}$ (kN) | 34.8 | 38.4 | 44.3 | 54.4 |
| Additional to Total Base Shear | 6.6% | 6.8% | 8.1% | 8.4% |

Elastic and damped design spectra are plotted in Fig.4. It is evident that the design point is located at the ascending branch (constant velocity period range), with minor differences being observed among irregular and regular frames. Since frame displacements are governed by drift limits, their design ductility demand is low ($\mu \approx 1.50$). Taller frames are inherently more flexible ($T_e \approx 3.8$s > 2.8s) and attract comparatively less base shear, including the added force for P-$\delta$ compensation ($R_v \approx 10\% < 13\%$).

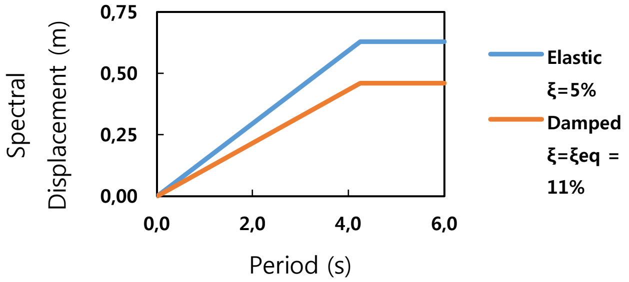


Fig. 4 Elastic and damped DDBD compatible design spectra

## 4. Structural Analysis in DDBD Design

As noted in the introduction and depicted in Fig. 5, two alternative design analysis methods have been proposed for the estimation of the required flexural capacity of the members. The first method includes conventional iterative or non-iterative linear structural analysis, with modeling assumptions conforming to the guidelines of Priestley *et al* (2007). On the other hand, the second method makes use of approximate hand calculations based on equilibrium.

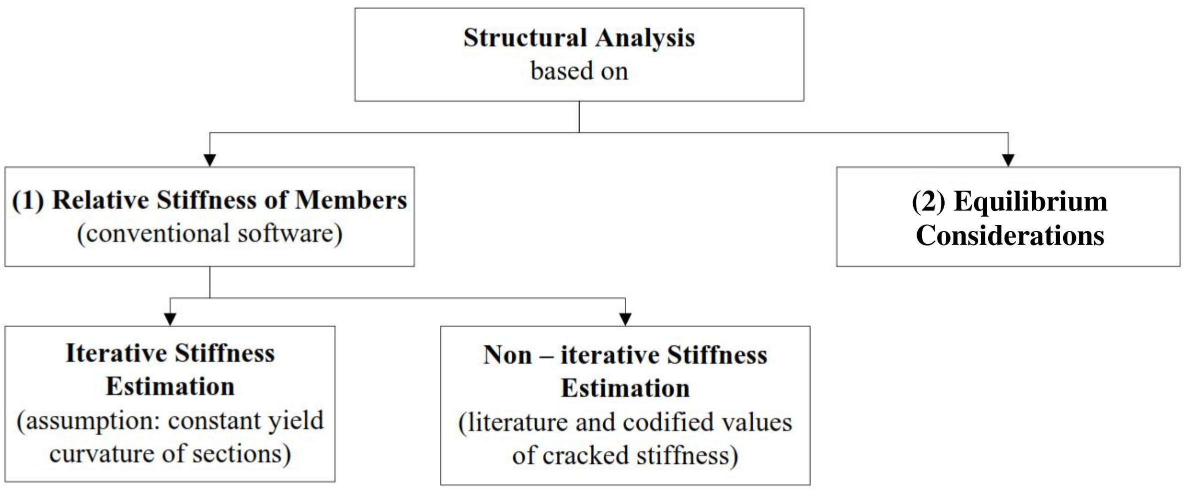


Fig 5 Available design analysis methods to accompany the DDBD method

### 4.1 Non iterative conventional design analysis

The difference of the conventional analysis methods, as far as their application using commonly available structural analysis software is concerned, lies in the effective stiffness values utilized for the beams. In line with the direct nature of the DDBD procedure, direct non-iterative analyses have been proposed, if reliable estimates of the cracked stiffness are employed. Such estimates can be found in Paulay and Priestley (1992), Priestley (2003) and currently enforced seismic design codes (EC8-1 2004, EC8-3 2005, KANEPE 2012). It should be noted, however, that since differences are observed among these proposed values, designers are encouraged to use the most up-to-date estimates of cracked stiffness.

### 4.2 Iterative conventional design analysis

While tabulated or codified values of the stiffness can be used, other approximate design analysis methods may also be employed, based on the yield curvature; the fact that constant yield curvature is a more realistic assumption for sections than constant effective stiffness (Priestley *et al* 2007), allows for incorporating this parameter into an iterative design process instead, such as the one described below, whereby the effective stiffness is iteratively obtained. Such an iterative method would seem a rational approach to apply, particularly in the case of unequal column sizes within the same storey, in view of the fact that irregular forms of setback structures are considered and columns do not carry the same gravity load. The procedure, depicted in the flowchart of Fig. 6, rather than using closed form expressions, iterates in order to obtain the correct value of the effective stiffness, since this depends on the member's flexural resistance, which is not readily available at the initial stage of the calculation. In order to estimate the effective member stiffness $I_{cr}$, the average moment $\overline{M}$ from both member ends is utilized, while yield curvature ($\varphi_y$) values are adopted from Sullivan *et al.* (2012) (Fig. 6).

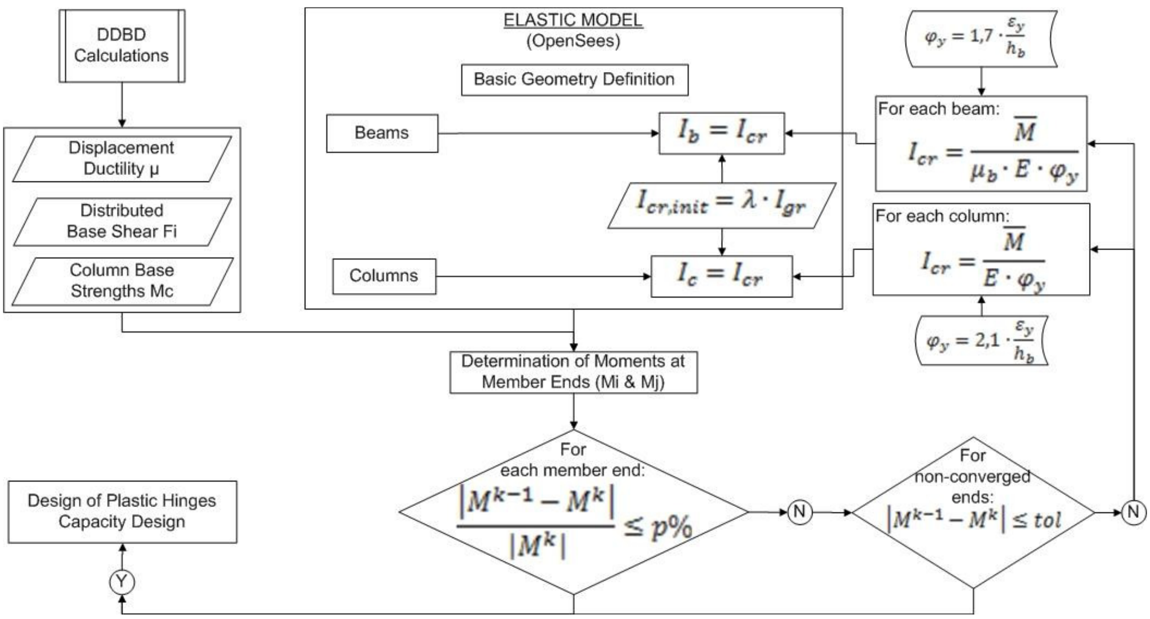

Fig. 6 Iterative structural analysis flowchart

### 4.3 Direct equilibrium design analysis

Regarding the second method of Fig. 5 (equilibrium considerations), its general outline is extensively described in the literature (Priestley *et al.* 2007). After the column base moments are identified, a bottom-to-top sequence of member equilibrium is followed to determine the required flexural strength in other locations. Nievas and Sullivan (2015) introduced a modification of the sequence to encompass the effect of setbacks at the corresponding joints. According to this procedure, the moment demand of the setback beam is equated with the moment of the concurring column, while the moments of the remaining beams, derived from equilibrium, are increased. Trial hand calculations by the authors showed that the increased demand of the other beams was comparable to the demand derived from the application of the conventional procedure in Priestley *et al.* (2007).

### 4.4 Critical examination of the conventional design of the Seven Storey Frames

In order to investigate the two conventional design analysis approaches described above, both the iterative and non-iterative conventional procedures were applied for the design of the Seven-Storey Frames in order to examine any differences in the member design outcome. For the iterative scheme, the relative and absolute difference tolerances were 1% and 1.0 kNm, respectively (Fig. 6). Both procedures were coded on the OpenSees platform (McKenna *et al.* 2010), since its scripting interface renders it extremely efficient in applying such unconventional iterative analysis procedures.

Given that for the Seven-Storey Frame A, inner and outer columns of the same storey had initially different dimensions, reflecting the differences in axial load due to the presence of the setback, it was observed that, the algorithm of the iterative procedure altered the load carrying behavior of the frames. Following the sequence of calculations described in Eq. (3) led the stiffer bays to fully attract the seismic forces, while the other members became seismically not critical. Step by step, the differences in stiffness were exaggerated, leading to excessive demands by the stiffer bays. Such a design procedure is naturally not apparent in the non-iterative analysis method, whereby the member effective stiffness remains constant.

$$h_1 < h_2 \Rightarrow \frac{1}{h_1} > \frac{1}{h_2} \Rightarrow \varphi_{y,1} > \varphi_{y,2} \Rightarrow \frac{1}{\varphi_{y,1}} < \frac{1}{\varphi_{y,2}} \Rightarrow (EI_{cr})_1 < (EI_{cr})_2 \tag{3}$$

Further analysis proved that the same design behavior was encountered in the irregular building as well, if non uniform member sizes were initially selected. As a result, the iterative procedure on constant yield curvature was deemed to be incapable of distributing equally the seismic load in cases of unequal column width, regardless of frame irregularity, as it can be deduced from the corresponding bending moment diagrams, derived from the iterative design analysis procedure, illustrated in Fig.7 (only the results of the outer frame are provided, since the inner frame's results were similar).

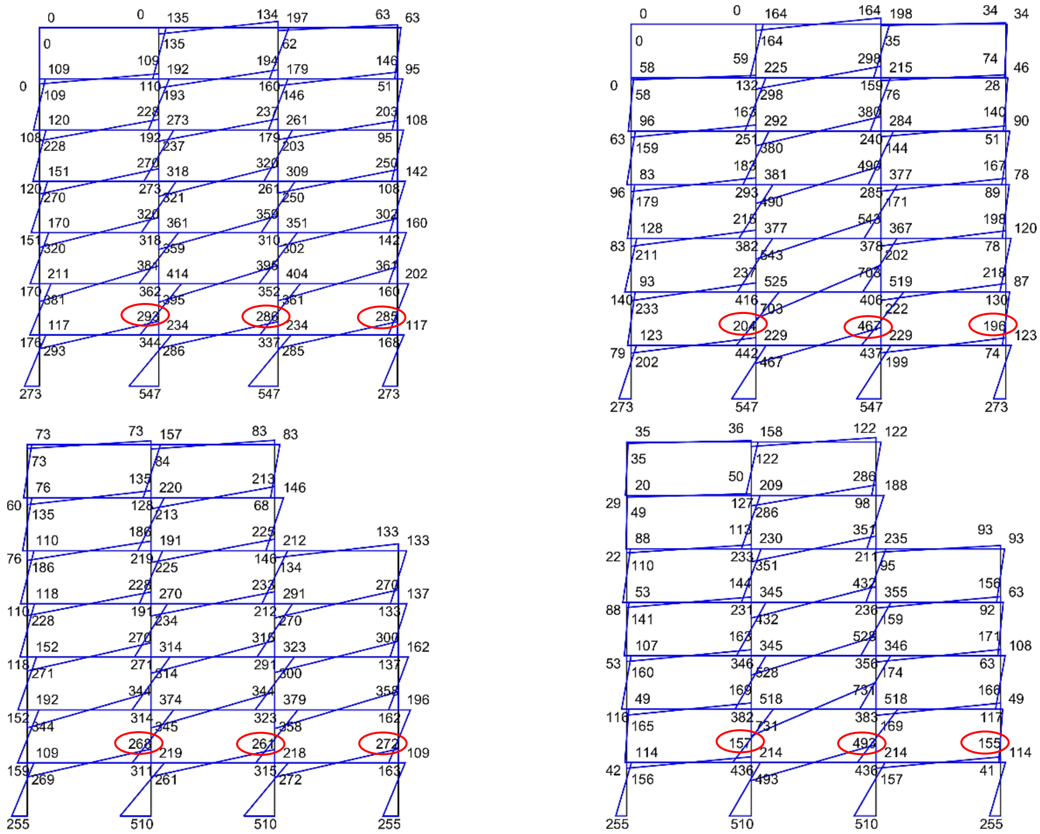

(a) (b)

Fig. 7 Bending moment diagrams for Seven-Storey Frames R and A with: a) uniform; and b) non-uniform column section dimensions.

It is additionally noted that similar behavior was observed during the design of the frames with unequal bay lengths, even with uniform sections. Stiffer bays (currently determined by beam lengths rather than column section dimensions) also attracted the majority of seismic loads, leading to unusual and doubtful designs. Consequently, equal dimensions for the columns in each storey were adopted in all cases considered. For completeness of the argument put forward, however, the two Seven-Storey Frame A designs using uniform or non uniform column configurations, are compared in detail under inelastic seismic response, in Section (8). It is expected that the frame with unequal bay capacities will demonstrate unfavorable seismic behavior, an issue further discussed in Section (8).

## 5. Detailing of Frame Member Sections and Inelastic Modeling

Having determined the required flexural strength at critical locations, the appropriate amount of reinforcement for all members is calculated. The influence of the iterative algorithm on section uniformity was tested on the Seven-Storey Setback Frame, where two configurations were designed. Detailing of plastic hinges and capacity design was applied according to the principles outlined in Section (3). Cross section dimensions and detailing of all frames are illustrated in Figs. A1 to A7, Appendix A. Characteristic concrete compressive strength was assumed equal to 30 MPa, while characteristic steel yield stress was taken equal to 500 MPa. Stirrup pattern and spacing were initially selected according to EC8-1 (2004) specifications and modified where needed. Specifically, the number of ties was determined by the number of longitudinal reinforcing bars, since the distance between two consecutive bars dictates that every rebar should be tied by transverse reinforcement.

Capacity design provisions for columns lead to more reinforcement than the amount necessary at the base plastic hinge. It is uncommon construction practice to put an increasing amount of reinforcement up the height of the column compared to the reinforcement at the base. Therefore, the largest number of reinforcing bars that is required at any column section is set at the column base and is curtailed along the column height as needed. Such a distortion to the design flexural strengths is unavoidable and is expected to affect the displacement profiles. In order to further investigate the influence of this practice, the Ten - Storey Frame R was also analyzed with reduced reinforcement at column bases. It is stressed out that this reduced amount, despite being closer to the design demands than initial detailing, was still necessarily increased; minimum reinforcement clauses still governed the design, even though for this case they were relaxed to 0,7% adopted, in lieu of 1% (EC2-1 2004).

The inelastic models of the frames were assembled in the OpenSees platform (McKenna *et al*. 2010) and non-linear static pushover (SPO) and dynamic time-history analyses (NLTHA) were carried out. Material model *Concrete01* was used for both unconfined and confined concretes, while material model *Hysteretic* was deemed appropriate for reinforcing steel. Confined concrete properties were calculated based on Eurocode 2 provisions (EC2-1 2004).
Beams and columns were modeled with distributed damage force-based *nonlinearBeamColumn* finite elements with five integration points. Frame joints were modeled with effectively rigid elastic elements. Diaphragmatic action was imposed with rigid truss members, instead of kinematic constraints of the respective degrees-of-freedom. It has

been reported that fictitious axial forces can be obtained in constrained elements with sections having asymmetric position of the neutral axis (Zeris *et al* (2007) and OpenSees online manual). To avoid such a distorted behavior, the modeling convention adopted in Zeris *et al*. (2007) were adopted, whereby double nodes were created and the beam axial degree-of-freedom only was released at one beam end. P-$\delta$ effects were accounted for in all the analyses. Following the recommendations by Priestley *et al.* (2007), 5% Rayleigh damping for NLTHA was assigned as tangent-stiffness proportional to the period of the fundamental mode, excluding mass – proportional terms. The first fundamental mode was calculated with OpenSees after the gravity loads were applied and cracking was initiated to the model. Special attention was also paid to the local behavior of members. The plastic rotation of member ends was compared with plastic rotational capacity, calculated according to EC8-3 (2005). It should be noted however that this comparison is indicative, since codified equations yield the chord rotation of members, including shear contribution and bar pullout.

For the NLTHA, a set of fourteen accelerograms was selected from the PEER NGA-West2 database (PEER 2014). Their selection was based on the moment magnitude and distance that characterize the design seismic scenario, while pulse-like records were avoided. A scaling factor was automatically computed, so that the mean response spectrum is well fitted with the Design Spectrum. The selected record characteristics and scaling are displayed in Table 2. The spectral displacements of the individual scaled records, as well as their mean spectrum are compared with the design spectrum in Fig 8.

Table 2 Selected characteristics of the ground-motion records used in NLTHA

| ID | Earthquake and Station Name | Year | Scale Factor | Magnitude | $R_{jb}$ (km) |
|---|---|---|---|---|---|
| 1 | Imperial Valley-02, El Centro Array #9 | 1940 | 1.9007 | 6.95 | 6.09 |
| 2 | Imperial Valley-06, El Centro Array #11 | 1979 | 1.5702 | 6.53 | 12.56 |
| 3 | Irpinia, Italy-01, Calitri | 1980 | 3.2386 | 6.9 | 13.34 |
| 4 | Corinth, Greece, Corinth | 1981 | 2.5486 | 6.6 | 10.27 |
| 5 | Kalamata, Greece-01, Kalamata (bsmt) | 1986 | 2.3315 | 6.2 | 6.45 |
| 6 | Superstition Hills-02, El Centro Imperial | 1987 | 1.7267 | 6.54 | 18.2 |
| 7 | Loma Prieta, Gilroy Array #4 | 1989 | 1.8076 | 6.93 | 13.81 |
| 8 | Northridge-01, W Lost Canyon | 1994 | 1.503 | 6.69 | 11.39 |

| | | | | | |
|---|---|---|---|---|---|
| 9 | Kobe, Japan, Shin-Osaka | 1995 | 2.1925 | 6.9 | 19.14 |
| 10 | Chi-Chi, Taiwan, CHY029 | 1999 | 2.0986 | 7.62 | 10.96 |
| 11 | Chi-Chi, Taiwan; TCU055 | 1999 | 1.8928 | 7.62 | 6.34 |
| 12 | Iwate, Japan, IWTH26 | 2008 | 1.1183 | 6.9 | 5.97 |
| 13 | El Mayor-Cucapah, El Centro Array #10 | 2010 | 1.5072 | 7.2 | 19.36 |
| 14 | Christchurch, Botanical Gardens | 2011 | 0.9914 | 6.2 | 5.52 |

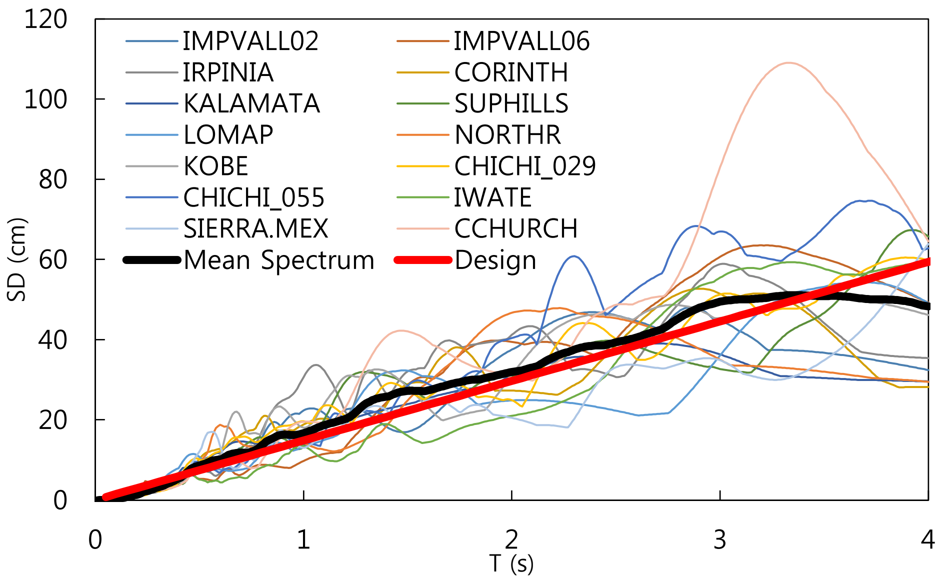


Fig. 8 Displacement spectrum of scaled records, mean spectrum and DDBD spectrum

## 6. SPO and NLTHA Analysis Results: Global Drift and Resistance Demands

The seismic behavior of the frames was evaluated by both global and local criteria. All response parameters have been established through SPO analyses and were subsequently compared with the average NLTHA envelope values. Global behavior in terms of total base shear and roof displacement is commonly been used in the literature as a criterion for the successful application of the design method. In the present study, local member ductility demands, imposed by frame displacements, were further addressed as well.

The SPO capacity curves depicted in Fig. 9 show a stable post-elastic behavior, apart from the Regular Ten-Storey Frame R. For this frame, the P-$\delta$ effects and the lower ductility supply associated with the relatively larger magnitude of gravity loads, led to unstable behavior with significant degradation of resistance. The overstrength factor $\Omega$ varied between 1.0 and 1.20. The average overstrength from the dynamic analyses was slightly increased

(1.25-1.50), while the maximum overstrength observed was 1.35 and 1.60, for the Seven-Storey and Ten-Storey Frames, respectively (both A and R). The maximum base shear is obtained at a roof displacement lower than the design value. It is evident that setback frames are less susceptible to P-$\delta$ effects than regular frames are. Furthermore, Ten – Storey Frame C, exhibits an even more stable behavior, owing to the relatively lower mass on the upper storeys. On the other hand, higher order effects are more influential on the behavior of Seven – Storey Frame B, than in the rest of the Seven – Storey frames. This phenomenon can be attributed to the more irregular geometric form of these frames. The amount and the distribution of the total base shear, as proposed by Eqs.(5.1), (5.8) and (8.1) of Sullivan *et al* (2012), are sufficient for counteracting these effects in terms of total base shear. Consequently, a stable behavior is generally achieved with reasonable overstrength factors for both the Regular and Setback structures.

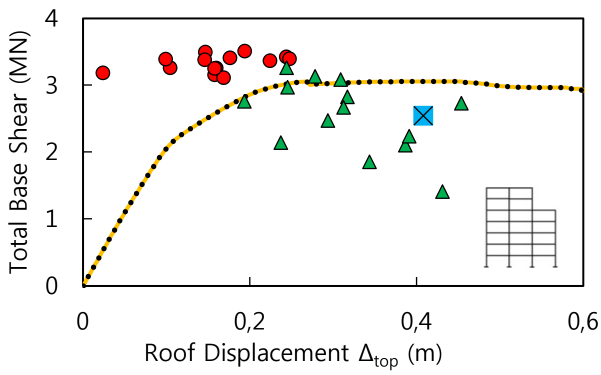


(a) Seven – Storey Frame A

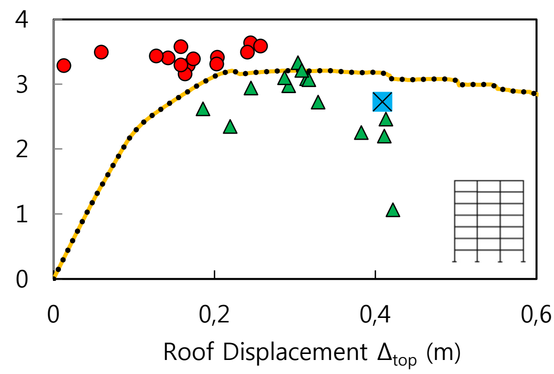


(b) Seven – Storey Frame R

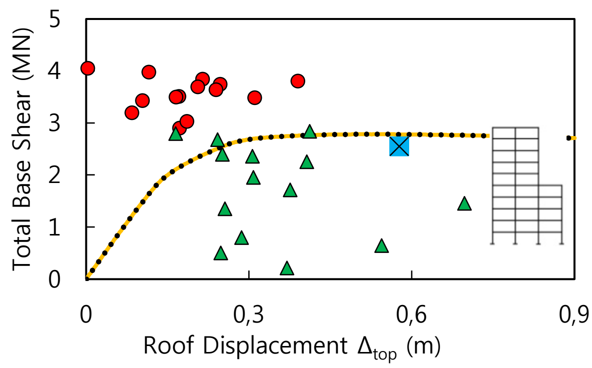


(c) Ten-Storey Frame A

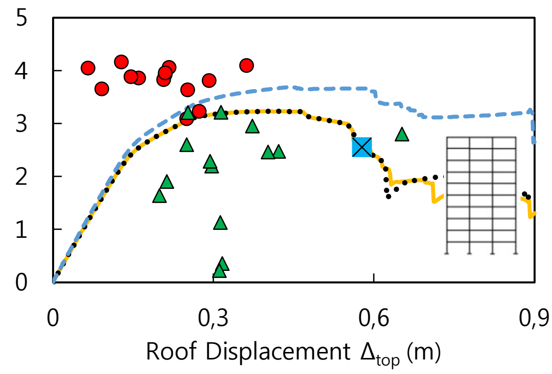


(d) Ten-Storey Frame R

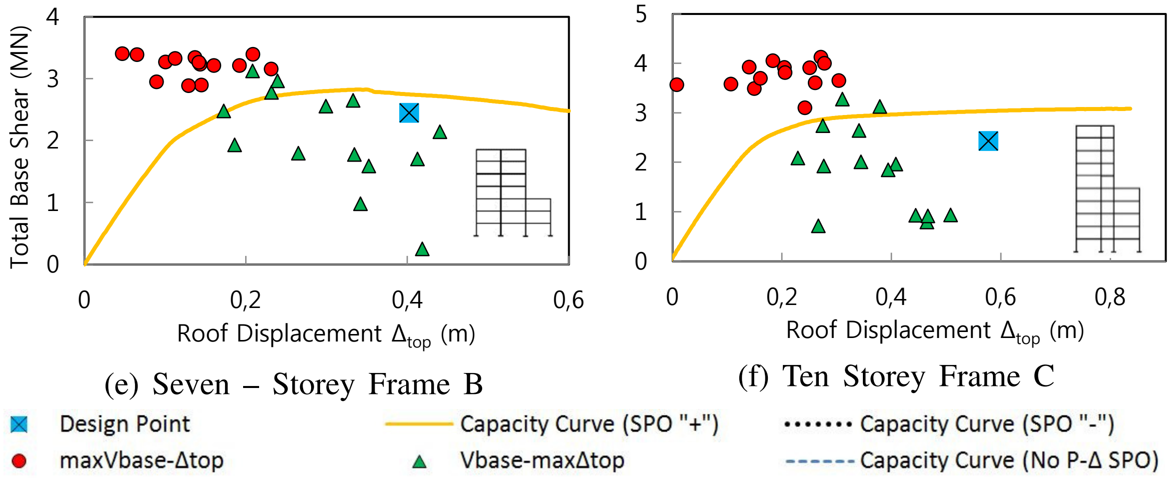

(e) Seven – Storey Frame B

(f) Ten Storey Frame C

Fig. 9 Comparison of the SPO capacity curves and the NLTHA peak base shear and roof displacement, all buildings and records considered.

Fig. 9 also depicts the envelope values from the NLTHA analyses (absolute values considered throughout). Both maximum base shear at the corresponding roof displacement and base shear at the instance of maximum roof displacement are shown. It is observed that the design roof displacement is rarely attained during NLTHA, whilst higher base shears and increased overstrength is developed by the frames. It is therefore attested that using the DDBD methodology together with the design displacement spectrum adopted, leads to conservative predictions of the irregular frames' roof displacement under NLTHA. Furthermore, it is observed that, generally, SPO predictions provide a median behavior to the NLTHA results in terms of base shear, which are more conservative in terms of roof displacement demand.

The drift profiles of the Seven-Storey and Ten-Storey Frames are depicted in Fig. 10. Maximum absolute values from individual NLTHA and their average are plotted, along with the corresponding SPO values at the , and are compared to the design profile. Since the design drift profile corresponds to the first inelastic mode of vibration, alterations are expected in the displacement profiles obtained from analyses due to higher modes contribution. Therefore, fundamental criterion for the success of the DDBD method is the non-exceedance of the maximum allowable drift of the design limit state, which has been previously defined as $\theta_c$= 2.5%. Even though Pettinga and Priestley (2005) observed good agreement between the design displacement profile and the NLTHA results of regular frames, more spurious results are obtained herein, especially for the Ten-Storey frames. This phenomenon is both attributed to record type and P-$\delta$ effects. Since natural accelerograms are scaled to match the design spectrum, a scatter in spectral demands exists throughout the period range; therefore, the various modes of vibration are expected to have different demands at different records, which will generally remain different as the structure softens.

The way P-$\delta$ effects modify response is similar to the behavior depicted on Fig. 9. In general, the displacements of the first levels are less than the design displacements. A plausible explanation lies with the fact that the reinforcement at the base of the columns is increased in order to comply with capacity design requirements of the upper levels. Thus, the lower part of the frame is made stiffer than the design assumptions and lower displacements are expected. It is also noted that SPO produces more conservative results than NLTHA, closer to the maxima than the average obtained values. The standard SPO is incapable of incorporating the higher mode effects at the response of the Ten-Storey Setback Frame, identifying the need of a more sophisticated procedure for such frames.

The drift profiles of the Seven-Storey Frames are in good agreement with the design drift profile, except for the first levels and the roof. The similarity of the SPO and the NLTHA results is also pointed out. The influence of the setback is not always evident, since both Regular and irregular type A frames exhibit similar behavior. On the contrary, setting the setback at a lower storey, as in Frame B, renders higher mode effects more important and imposes higher drifts on the upper storeys. This influence of higher modes is more apparent at the Ten-Storey Frames. Drifts are initially increasing with setback height, leading to significant excess of the design values in the middle and upper parts of the Ten Storey frames, especially in Ten Storey Frame A.

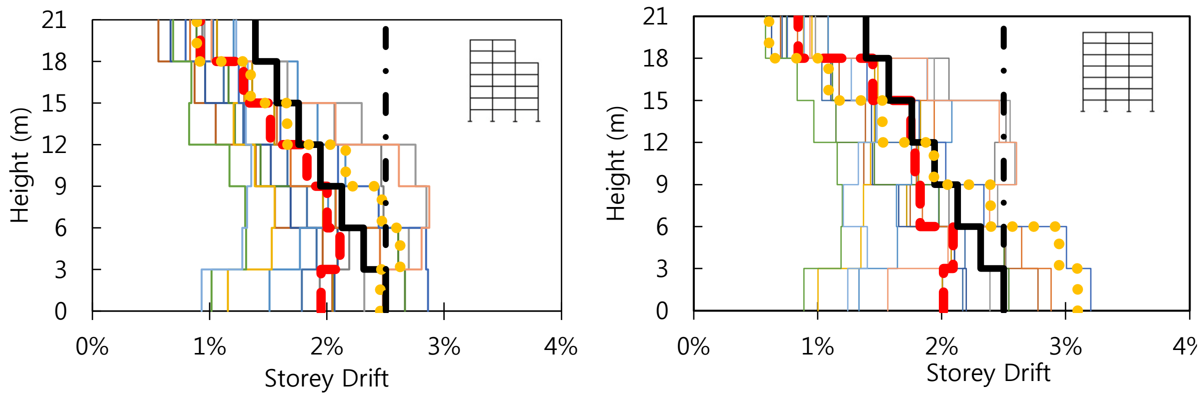


(a) Seven–Storey Frame A (b) Seven–Storey Frame R

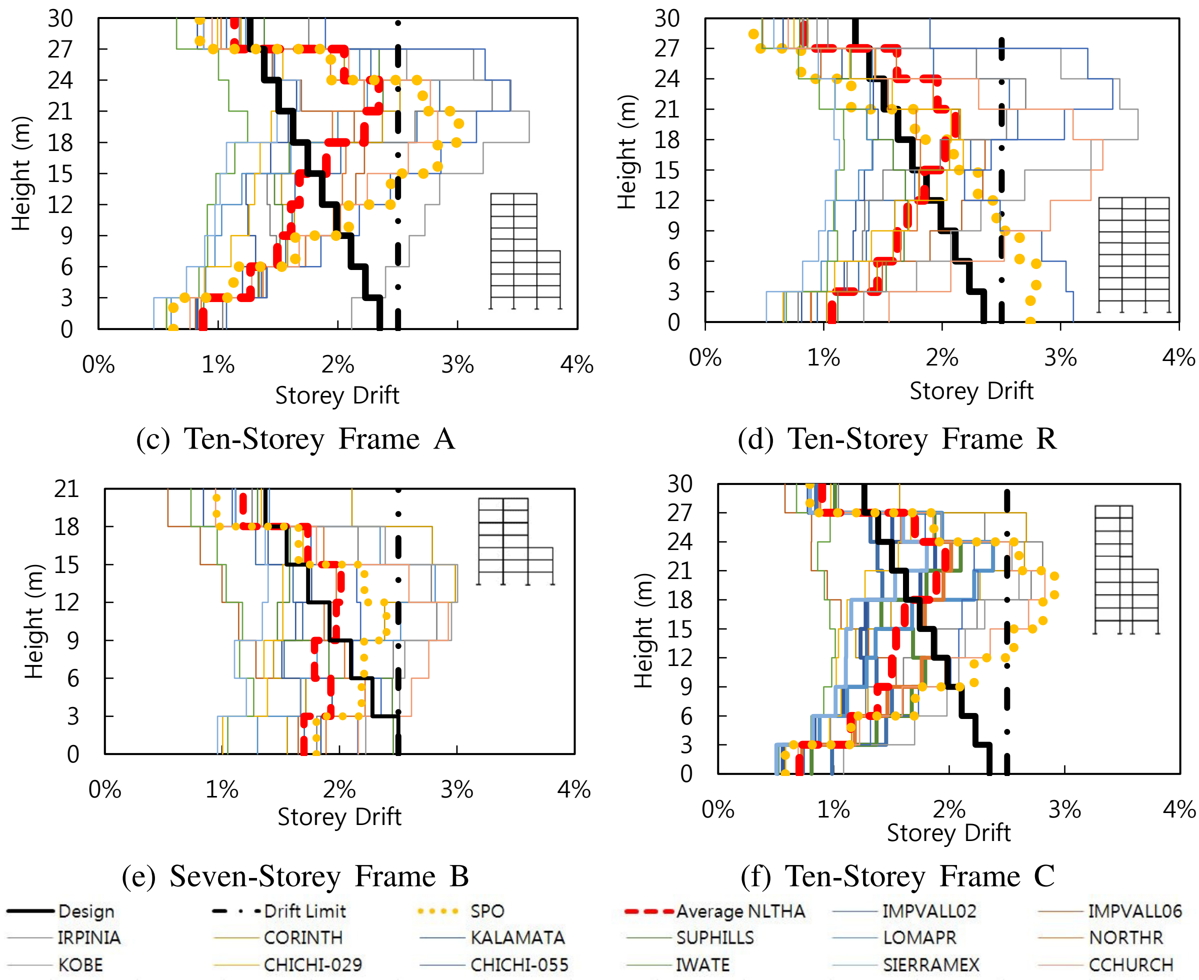


Fig. 10 Comparison of the peak absolute drift profiles under NLTHA, with design limit and SPO prediction at the design roof deformation, all buildings and records considered.

Ten – Storey Frame 10C exhibits storey drifts at the upper storeys that are less than their counterparts of Frame A, a behavior that could be anticipated from the capacity curves. Absolute drifts are constantly lower than the design values. The average NLTHA response of all frames does not exceed the 2.5% limit, in terms of drift. Therefore, the drift reduction factor $\omega_\theta$ used for design does not need modification. In conjunction with this observation, together with the predicted capacity curves, it can be concluded that handling of P-$\delta$ and higher mode effects at the global level is sufficient both for regular and irregular RC frames considered.

The storey shear profiles of the Seven-Storey and the Ten-Storey Frames are illustrated in Fig. 11. For simplicity, only the shear forces of the inner frame columns are shown. The average column shear forces obtained by NLTHA are in excellent agreement with the capacity design assumptions, while SPO results underestimate their magnitude, a finding that is consistent with the base shear plots of Fig.9; this is attributed to the fact that the imposed lateral force profile under SPO, for these irregular frames, does not necessarily correspond to the inertia force profiles during dynamic response under NLTHA. In some cases, the envelope shear forces are also well predicted. The inherent conservatism of Eq. (9.5) of Sullivan *et al* (2012) for tall regular frames has been attested by Priestley *et al.* (2007), but this safety margin is shown to be sufficient to cover the shear amplification for the irregular frames. Shear failure was avoided at every analysis. In fact, the margin between shear demands and dependable shear strength was significant, since the detailing rules that are enforced by codes were taken into account during shear design; the provided stirrup spacing was governed by avoidance of buckling of the longitudinal reinforcement. It is stressed out that Priestley's *et al* (2007) suggestion is stricter than Eurocode limits.

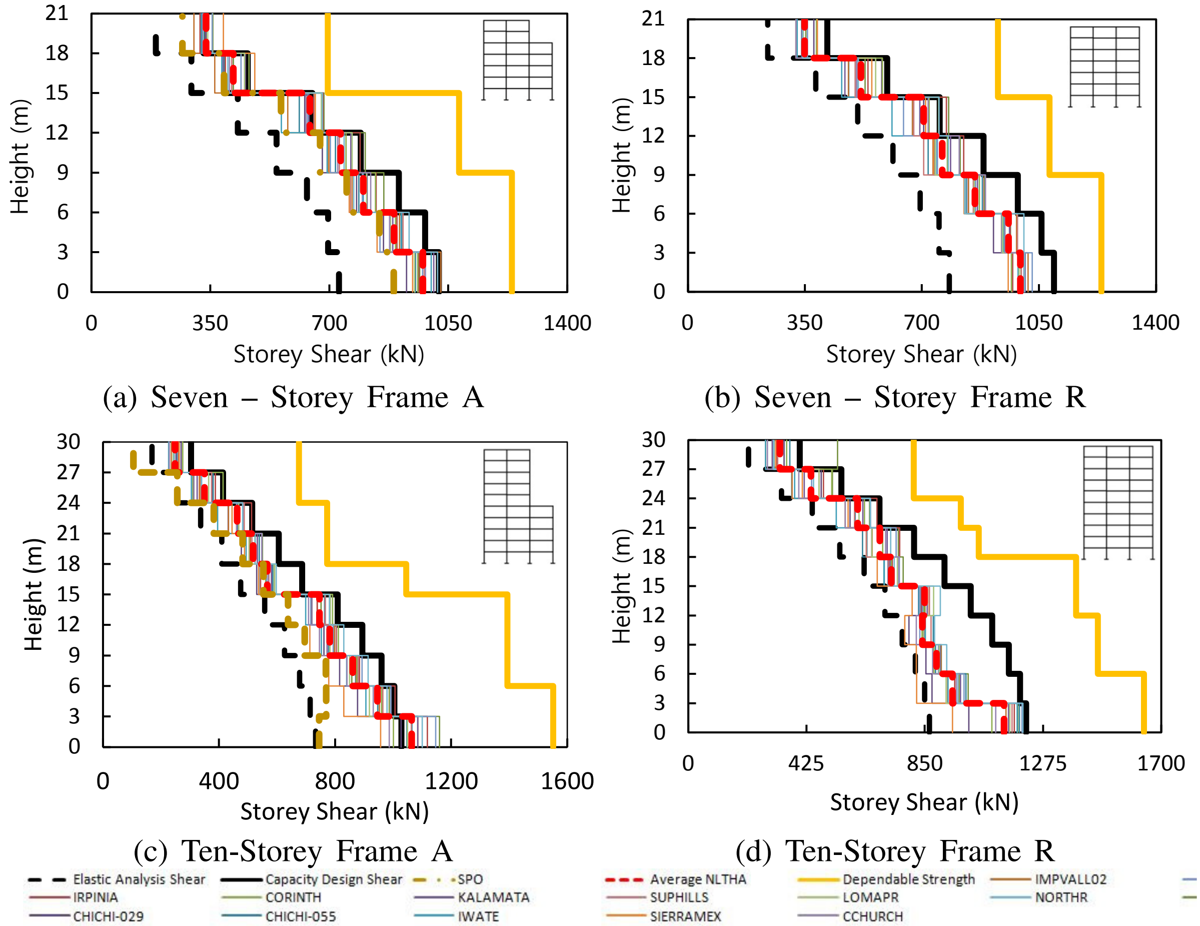


Fig. 11 Comparison of the storey shear profiles under NLTHA with design and SPO at the design roof deformation, all buildings (interior frames) and records considered.

## 7. SPO and NLTHA Analysis Results: Implications on Local Member Demands

Attention is now drawn to the local level in order to identify if the global displacement demands cause depletion of the local ductility capacity. Implications of global demands to the local level are important, since the achievement of the design performance level (i.e. the formation of a favorable collapse mechanism within the prescribed drift limits) depend on the condition of no failure at the local level, i.e. plastic rotation demands do not exceed the plastic rotation capacity. Both average maximum values and the development of plastic rotations are hereafter considered.

The average value of the maximum absolute plastic rotations obtained from NLTHA at each plastic hinge is depicted graphically in Fig. 12a (again, only the inner setback frames are shown for clarity). The percent total hysteretic energy absorbed separately by the beams and columns of each storey, is illustrated in Fig.12b. Since no exact values are plotted, these figures provide a more qualitative approach; the formation of the prescribed collapse mechanism (beam-sway) is attested and the sections that absorb more hysteretic energy are identified. The spatial distribution and magnitude of the plastic rotations appear strongly correlated with the drift profile. It is noted that the regular ten-storey frame utilizes middle height beams and upper storey columns significantly more than the respective setback frame that is depicted in Fig. 12. Capacity design has been successfully implemented since insignificant plastic deformations were observed at columns. Therefore, Eq. (9.2) of Sullivan *et al* (2012) seems to sufficiently enforce the as predicted hinge distribution in the beams, and therefore needs no modification.

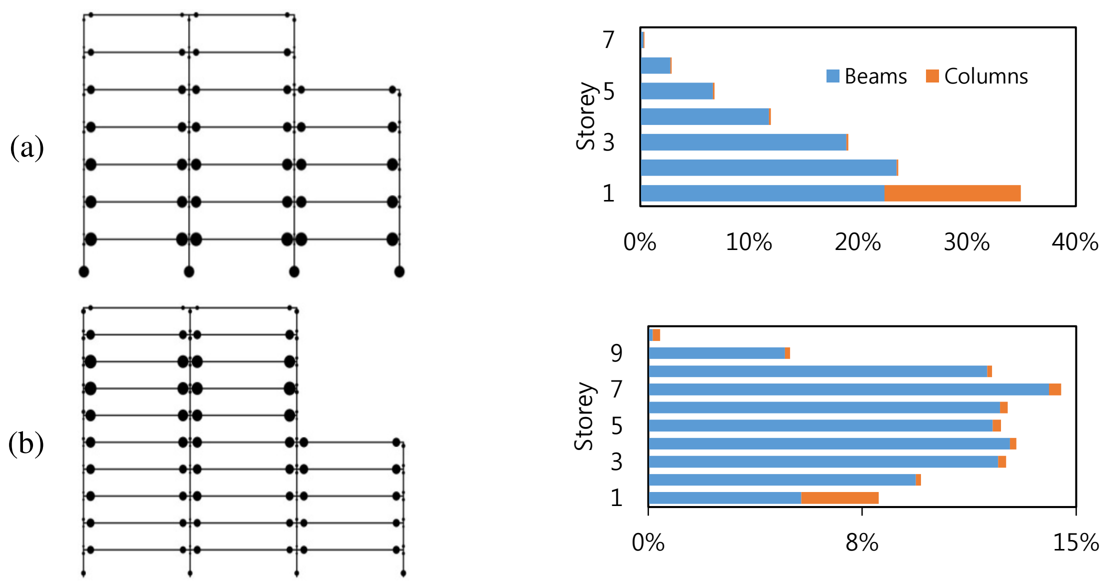


Fig. 12 Distribution of plastic hinges (Left) and hysteretic energy absorption (Right) of: a) Seven-Storey Frame A and; b) Ten-Storey Frame A

Apart from the formation of a suitable collapse mechanism, essential are the checks confirming that the plastic rotational capacity has not been exceeded. Fig. 13 illustrates the development of plastic rotations during SPO at characteristic locations (continuous line), along with the envelope values of NLTHA (dashes and crosses), compared to the rotational capacity (dashed line, following EC8 – 3 2005, KANEPE 2012) and the design plastic rotation (square point). In order to maintain the clarity of the plots, only the maximum plastic rotations are plotted. The values depicted correspond to the beam end under negative bending, because they are more critical due to the influence of gravity loads on the shear span's length. Similar to Fig. 9, both the maximum plastic rotation with the corresponding roof displacement (dashes) and the plastic rotation at the instance of maximum roof displacement (crosses) are depicted. In order to provide a better comparison between local and global behavior, plastic rotations are also plotted against the corresponding storey drift – a more localized global deformation parameter, compared to the roof displacement. It is also noted that the scatter from the monotonic trend is in this case reduced, compared with the results plotted against the roof displacement, thus validating the use of the storey drift as a reliable index of local damage for the case of irregular buildings.

Depletion of the rotational capacity was often observed in members that were subjected to increased demands, such as base columns and first-storey beams. Since codified equations include fixed-end rotations and shear deformations (EC8 – 3 2005, KANEPE 2012), failure would be expected to be much more imminent than what these figures imply. The increase of

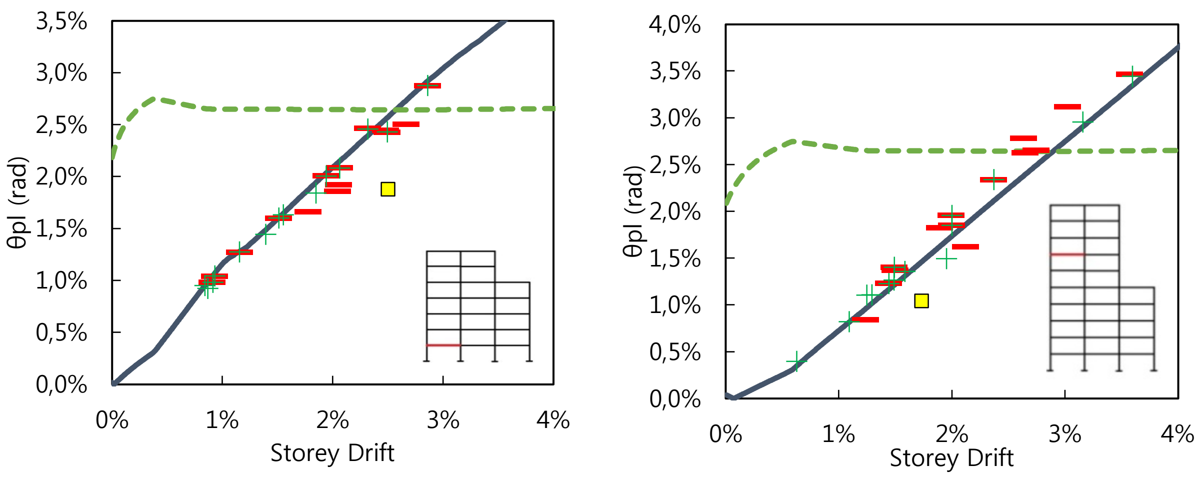


(a) Seven-Storey Frame A

(b) Ten-Storey Frame A

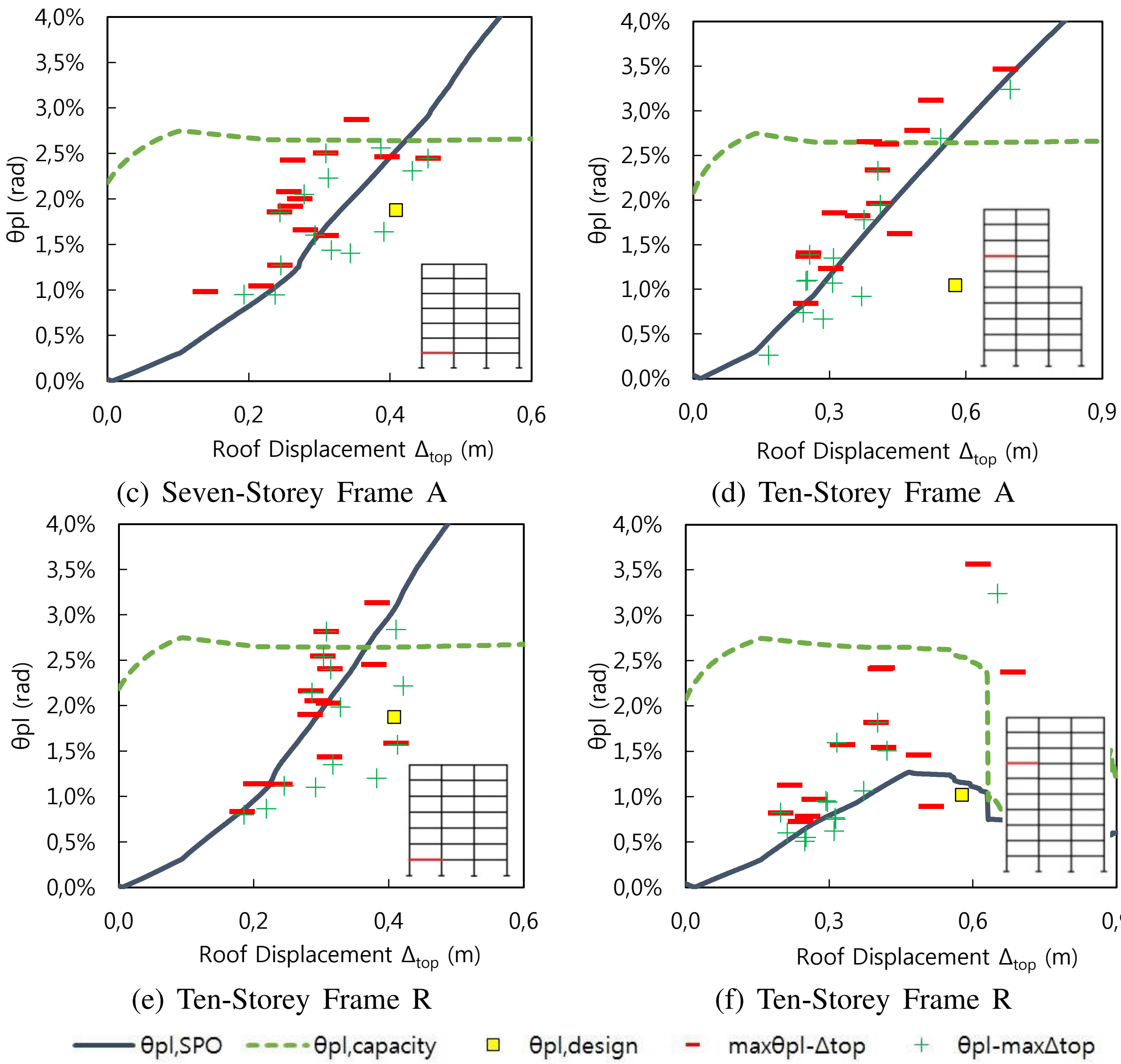


Fig. 13 Development of plastic rotations in the building beams in terms of: a) and b) the corresponding storey drift and; c) to e) the roof displacement

plastic rotation demands with reference to roof displacement, as obtained by NLTHA, displayed a tendency that was effectively described by the static SPO. An exception to this rule was posed by the Ten-Storey Frame R, where plastic rotation demands accumulated earlier than predicted by SPO. The situation has been anticipated and is in line with the disharmony between displacements and the global instability of that structure, which has been previously noted. Furthermore, the departure of drift demands from the drift design profile is in line with the difference between design plastic rotation and analysis results. Even though in terms of drift, the outcome was not severe, because ultimately there was conformation with the drift limit of the limit state, this is not the case for plastic rotations; Failure can be imminent, therefore jeopardizing the whole structure’s response, while the designer is not aware of the exceedance that could be accommodated during the design. It is also pointed out that the response of the 10storey frame with the reduced reinforcement at column bases is effectively the same with its regular counterpart with unreduced reinforcement; the reduction of moment capacity at the bases is not enough to alter the global behavior in terms of drift. On the contrary, the frame is susceptible to soft storey failure at ground floor; Plastic rotations of the upper end of the ground floor column are doubled, when compared to their regular counterpart and become comparable to those at the base, where a hinge formed.

The influence of unequal bay lengths on local demands is now examined, considering the Ten – Storey Frames, types B – C and D. After evaluation of the SPO and NLTHA results, it is concluded that the global behavior in terms of drift remains unaffected by the shorter span frame and bears similarity with their equal – bay counterparts. Fig. 14 illustrates the development of plastic rotations from SPO (continuous line) and the NLTHA maxima (dashes and crosses), compared with the rotational capacity (dashed line) for a long and a short beam at the $6^{th}$ storey (Figs. 14a and 14b, respectively). At first, it is observed that the local demands on shorter beams do not significantly differ from the demands on longer beams and therefore cannot provide the basis for a rule, without further investigation. During SPO, the similarity was anticipated, since a beam-sway mechanism is practically enforced. Furthermore, the development of plastic rotations during SPO is characterized by a linear trend, which is further validated by the maxima points of the NLTHA. The discrepancies between design predictions and analysis demands that have been identified for drifts are also valid for plastic rotations, signaling an overestimation of plastic rotation at the lower and an underestimation at the upper storeys, respectively. Depletion of rotation capacity is noted as well, especially at the upper storeys. It is also noted that insignificant differences at the seismic behavior where observed, when the external left bay was shortened instead of the central.

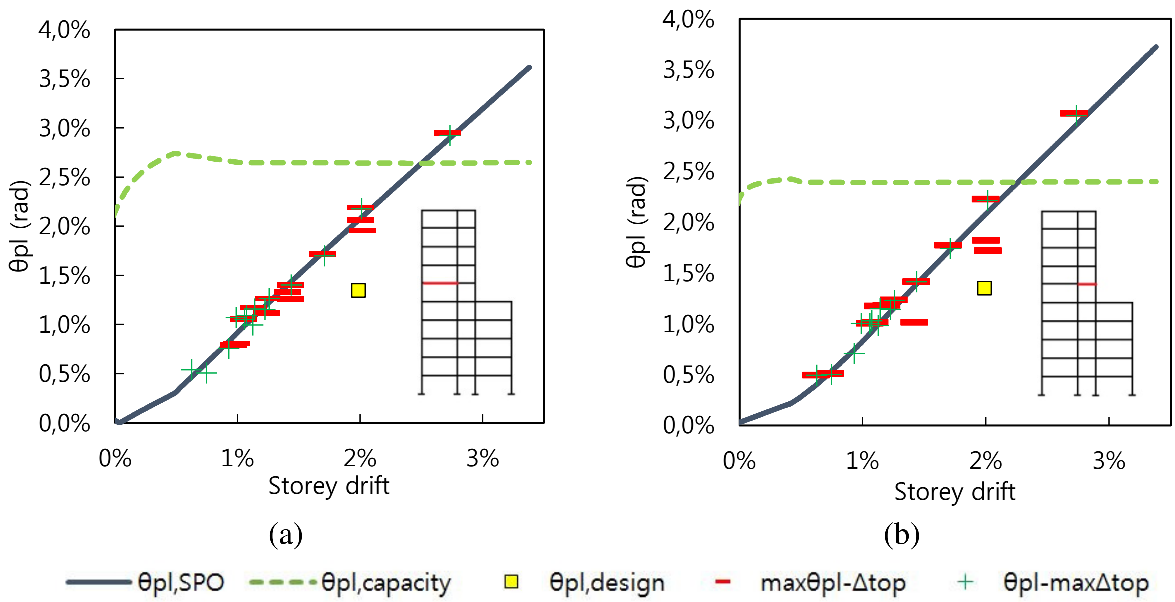


Fig. 14 Development of beam plastic rotations of Ten-Storey Frame C, at: a) The longer span; and b) The shorter span.

In order to further investigate the effect of height irregularity, the setback storey at the Seven – Storey Frames is set at the 3rd storey instead of the 5th. Thus, the upper part of the frame has formed a tower, where higher mode effects are expected to be more significant. Fig. 15a depicts the development of plastic rotations at a 4th storey beam along with the maxima points of NLTHA for this case. It is observed that the trend of the SPO is still validated by the NLTHA, albeit with higher scatter in the demands. It is further noted that the many NLTHA maxima are accompanied with an increased storey drift exceeding the 2.5% design limit, a phenomenon that was less frequently observed in the other case buildings studied. The design plastic rotation is once again underestimated and the tower beams are more utilized than expected. This finding is attested by Fig 15b, where the hysteretic energy absorption is depicted. Increased amounts of energy are absorbed by the beams of the tower, especially when compared to Fig 12a-(right), which represents a more regular behavior; Seven – Storey Frame C absorbs energy more uniformly, while Frame A shows a triangular distribution.

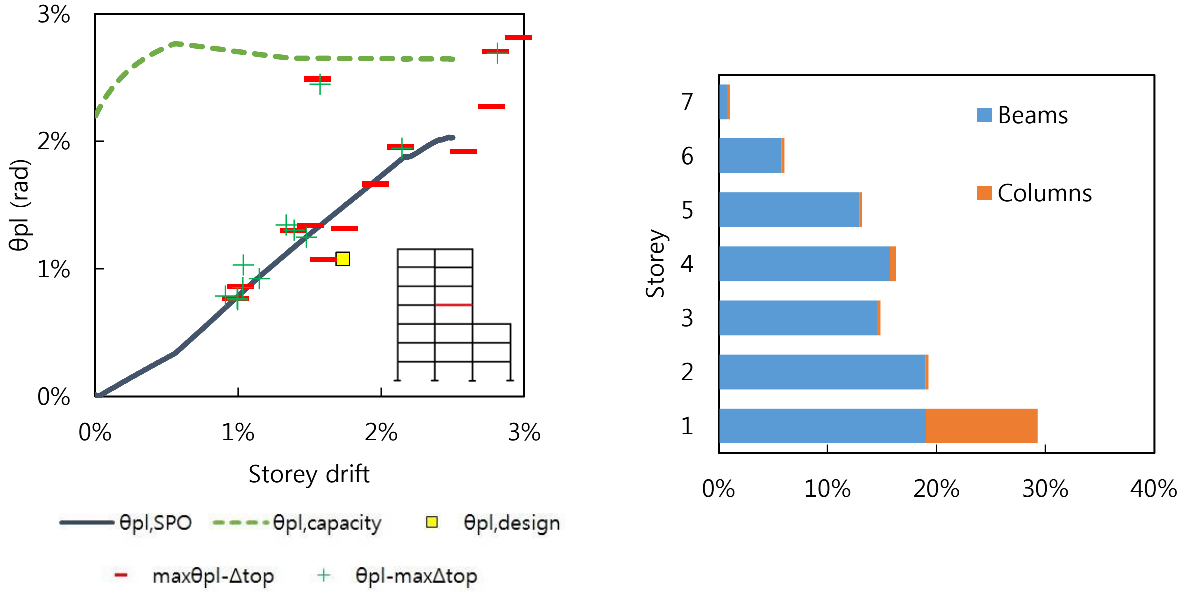


(a) (b)

Fig. 15. Seven-Storey Frame C (Tower): a) Development of beam plastic rotations; and b) Hysteretic energy absorption with height

A similar behavior was encountered at the profile of increasing vertical interstorey drifts with roof displacement, but the presented figures are more informative, because of the presence of an upper bound indicative of failure. Plastic rotational and drift demands differ from their respective design values in a similar manner.

## 8. Performance of the Frame with Non-Uniform Column Section Dimensions

So far, only the frame configurations with uniform sections have been considered. Figs. 16 – 17 summarize the response of the Seven-Storey Setback Frame with the adoption of non-uniform column dimensions and designed using the iterative conventional analysis described in Section (4.2). It is apparent that a frame designed according to such principles exhibits an unfavorable behavior and is susceptible to soft storey at the setback level (Fig. 16a). Shear failures are also observed, since both single NLTHA and average behavior shows that shear demand overrides the dependable strength (Fig. 16b). For these failures to be avoided, stirrup configurations denser than design requirements were assumed, as shown in Fig. A1.

In terms of total base shear, significant overstrength ($\Omega \approx 2.0$) was observed. The drift profiles are constantly increasing with height, signifying a stiff behavior characteristic of wall-type structures rather than frames (Fig. 16a). They also significantly deviate not only from the design drift profile, but also from the drift limit, thus implying relatively higher damage in this structure than intended by the design performance level. Furthermore, as can be seen from the spatial distribution of plastic hinges in Fig. 17a, hysteretic energy was absorbed in a limited number of cross-sections, while, their rotational capacity was exceeded in several nonlinear dynamic analyses (Fig. 17b). Thus, the disharmony between design predictions and analysis results that is apparent in drift profiles is also observed in the member local behavior.

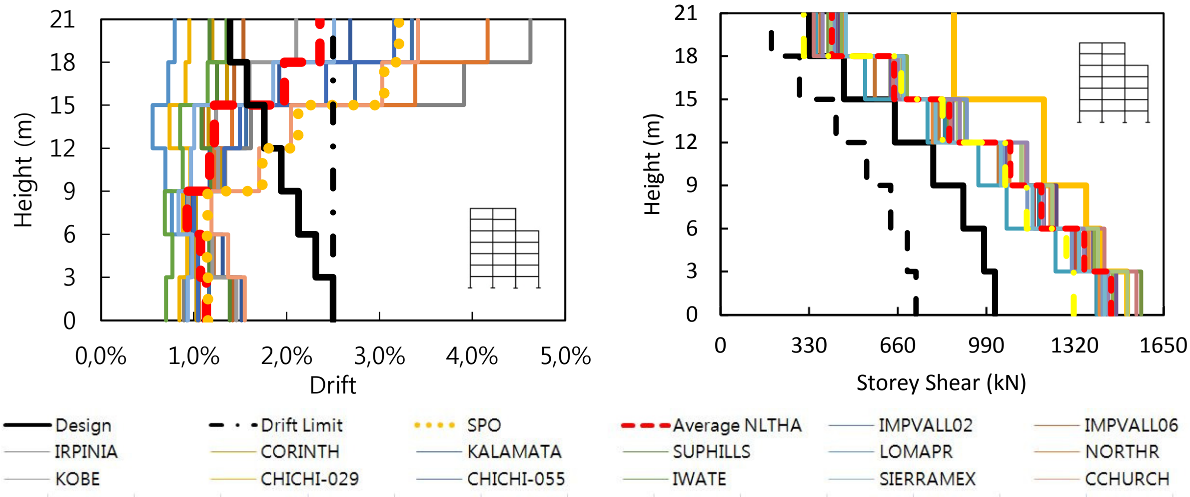


(a) (b)

Fig. 16 Seven-Storey Setback Frame with non-uniform sections: a) Drift profiles and; b) Storey shear

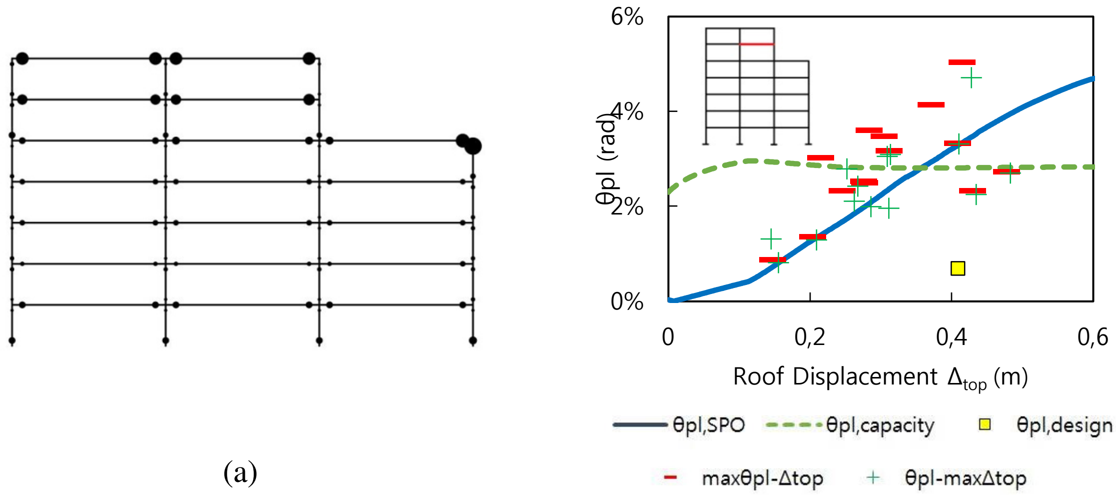


(a) (b)

Fig. 17 Seven-Storey Setback Frame A with non-uniform column section dimensions: a) Plastic rotation spatial distribution and; b) Development of a typical beam's plastic rotation under SPO and NLTHA (for notation, see Fig. 18).

## 9. Conclusions

The DDBD method has been applied to the design of several in height regular or irregular setback RC frames seven and ten stories tall, with different numbers of recessed stories and span irregularity. All structures were subsequently analyzed as plane frames under nonlinear SPO and NLTHA analyses, using a set of fourteen base excitations. Considering the global and local performance of the case structures, the following are concluded:

- With minor exceptions for the tall setback configurations, the peak roof displacement demand under NLTHA did not exceed the design roof displacement adopted in the DDBD design of the frames using the damped DDBD compatible design spectra proposed in Priestley *et al.* (2007).

- Even though the influence of higher modes and P-$\delta$ effects were considered in design, their contribution to the response introduced significant deviations from the design drift profiles observed by the NLTHA predictions, particularly for the Ten Storey Frames. The maximum allowable drift for the design limit state, namely 2.5% was not, on average, exceeded for all fourteen NLTHA, thus confirming the success of the design in terms of drift. However, considerable scattering deviation by as much as 200% of the design anticipated value was obtained at the upper third of the buildings studied and for selected ground motions, with most notable differences obtained in the case of the Ten – Storey Setback and Regular frames.

- The SPO capacity curves of the buildings indicated an acceptable behavior and the preservation of instability at acceptable levels. Therefore, the treatment of higher modes and P-$\delta$ effects, as is currently incorporated into DDBD design, is satisfactory for the cases considered. However, based on the analysis findings, it is concluded that the taller regular frames were more susceptible to P-$\delta$ effects than the corresponding setback frames. Additionally, the calculation of the required shear strength, as is currently enforced in DDBD, was conservative enough to account for the shear amplification observed in the irregular frames.

- Capacity design provisions were also proven to be sufficient for the irregular frame designs, since no significant column hinging was observed apart from the base critical region at the ground storey. Furthermore, no column hinging was observed at the recess levels. Weak beam – strong column collapse mechanism was successfully enforced at all cases, leading to a more stable behavior; inelastic behavior is limited to the inherently more ductile members, namely the beams.The interrelation between local (member) and global (e-SDOF structural) ductility demands requires further development, for better control of the local damages incurred at the ultimate limit state design displacement. It has been repeatedly observed in the analyses herein that global e-SDOF displacements, characterizing the design limit state, led to excessive local plastic rotation ductility demands that did not conform with the design limit state assumptions, leading many members to exhibit premature failure due to depletion of their plastic deformation capacity. Therefore, not only the subsequent limit state (collapse prevention) was more imminent than intended, but the achievement of the design limit state in itself (repairable damage) may be questionable. Further investigation is also needed for a more accurate establishment of the beams' design plastic rotation; their values have been repeatedly underestimated, a phenomenon that is consistent with the exceedance of the design drift.

- On the other hand, investigation of the local demands induced for the different forms of irregularity show insignificant correlation between them. For the cases considered, setbacks with both equal or unequal bay lengths do not significantly alter the plastic rotation demands on the beams, when compared to the regular configurations. Given the limited amount of data, however, further investigation is needed, where other configurations, taller and relatively slender building forms and additional types of geometric irregularity can be examined (e.g., other tower forms, frames with discontinuous beams or columns), before the establishment of a general design rule.

- An extensive comparative study of the alternative methods for linear structural analysis showed that the iterative conventional procedure is inadequate for the design of frames whose stiffness is inherently non – uniformly distributed. Such are the cases of unequal column dimensions or unequal bay lengths within the same storey. Stiffer bays attracted the majority of the seismic load, regardless of the irregularity of the frame. The seismic behavior of such frames was unacceptable, since drift limits and deformation capacity were often exceeded, while they were found to be susceptible to a soft storey collapse mechanism and shear failures. Consequently, the only viable solution for the rational design of such frames – apart from equilibrium considerations – is the adoption of realistic estimates of the cracked stiffness in non-iterative analyses.

## References


Akkar, S. and Bommer, J.J. (2007) "Prediction of elastic displacement response spectra in Europe and the Middle East", *Earthquake Engng Struct Dyn,* **36**,1275-1301

Amiri, G. G., Shalmaee, A. M. and Namiranian, P. (2016) "Evaluation of a DDB design method for bridges isolated with triple pendulum bearings", *Structural Engineering and Mechanics*, **59**(5), 803-820.

Cardone, D., Palermo G. and Dolce M. (2010) "Direct Displacement-Based Design of Buildings with Different Seismic Isolation Systems", *Journal of Earthquake Engineering*, **14(2)**, 163-191.

Cauzzi, C., Faccioli, E., Paolucci, R. and Villani, M. (2008), "Long – Period Ground Motion Evaluation from a Large Worldwide Digital Strong Motion Database", *14$^{th}$ World Conference on Earthquake Engineering,* Beijing, China

EC2-1 (2004), EN 1992-1-1:2004, Design of Concrete Structures – Part 1: General Rules and Rules for Buildings, European Committee for Standardization, Brussels, Belgium.

EC8-1 (2004), EN 1998-1:2004. Design of Structures for Earthquake Resistance – Part 1: General Rules, Seismic Actions and Rules for Buildings, CEN, Brussels, Belgium.

EC8-3 (2005), EN 1998-3:2005. Design of Structures for Earthquake Resistance – Part 3: Assessment and retrofitting of buildings, CEN, Brussels, Belgium.

Faccioli, E., Paolucci, R. and Rey, J. (2004), "Displacement spectra for long periods", *Earthquake Spectra*, **20**(2), 347-376.

Gkatzogias, K. and Kappos, A. (2015) "Deformation-based seismic design of concrete bridges", *Earthquakes and Structures*, **9**(5), 1045-1067.

KANEPE (2012), Code of Structural Interventions, Earthquake Planning and Protection Organization of Greece, Athens, Greece.

Inel, M. and Meral, E. (2016) "Seismic performance of RC buildings subjected to past earthquakes in Turkey", *Earthquakes and Structures*, **11**(3), 483-503.

Landi, L., Pollio, B., and Diotallevi, P. P. (2014) "Effectiveness of different standard and advanced pushover procedures for regular and irregular RC frames", *Structural Engineering and Mechanics*, **51**(3), 433-446.

McKenna, F., Scott, M. H., and Fenves, G. L. (2010) "Nonlinear Finite-Element Analysis Software Architecture Using Object Composition," *Journal of Computing in Civil Engineering*, Vol. 24, No.1, pp. 95–107.

Malekpour, S., Ghaffarzadeh, H., and Dashti, F., (2013). "Direct displacement-based design of steel-braced reinforced concrete frames". *Structural Design of Tall and Special Buildings*. **22**(18), 1422-1438.

Mergos, P. E. (2013) "The anchorage-slip effect on direct displacement-based design of R/C bridge piers for limiting material strains", *Computers and Concrete*, **11**(6), 493-513.

Muljati, I., Kusuma, A. and Hindarto, F. (2015), "Direct displacement based design on moment resisting frame with out-of-plane offset of frame", *Procedia Engineering*, **125**, 1057 – 1064

NGA-West2 (2014), PEER Ground Motion Database, Pacific Earthquake Engineering Research (PEER) Center, Berkeley, CA, USA, http://ngawest2.berkeley.edu

Nezhad, M. E., and Poursha, M. (2015) "Seismic evaluation of vertically irregular building frames with stiffness, strength, combined-stiffness-and-strength and mass irregularities", *Earthquakes and Structures*, **9**(2), 353-373.

Nievas, C.I. and Sullivan, T.J. (2015), "Applicability of the direct displacement-based design method to steel moment resisting frames with setbacks", *Bull. Earthqu. Eng.*, **13**(12), 3841-3870.

O'Reilly, G. J., Sullivan, T. J., and Filiatrault, A. (2017) *"Implications of a More Refined Damage Estimation Approach in the Assessment of RC Frames,"* 16th World Conference on Earthquake Engineering, Santiago, Chile

Paparo, A. and Beyer, K. (2015) "Development of a displacement-based design approach for modern mixed RC-URM wall structures", *Earthquakes and Structures*, **9**(4), 789-830.

Pettinga, J.D. and Priestley, M.J.N. (2005), "Dynamic behaviour of reinforced concrete frames designed with direct displacement-based design", *J. of Earthqu. Eng.*, **9**(2), 309-330.

Paulay, T. and Priestley, M.J.N. (1992), *Seismic Design of Reinforced Concrete and Masonry Buildings*, Wiley, New York.

Pennucci, D., Sullivan, T.J. and Calvi G.M., *Displacement Reduction Factors for the Design of Medium and Long Period Structures, J. of Earthqu. Eng.*, **15**(1), 1-29.

Priestley, M.J.N. (2003), *Myths and Fallacies in Earthquake Engineering, Revisited, The 9$^{th}$ Mallet Milne Lecture*, IUSS Press, Pavia, Italy.

Priestley, M.J.N., Calvi, G.M. and Kowalsky, M.J. (2007), *Displacement-Based Seismic*

*Design of Structures*, IUSS Press, Pavia, Italy.

SEAOC. (1995) Vision 2000: Performance-based seismic engineering of buildings, Sacramento, California

Sullivan, T.J., Priestley, M.J.N. and Calvi, G.M. (2012), *A Model Code for the Displacement-Based Seismic Design of Structures DBD12*, IUSS Press, Pavia, Italy.

Takeda T., Sozen M. and Nielsen N. (1970). "Reinforced Concrete Response to Simulated Earthquake", *Journal of the Structural Division*, ASCE, **96**, 2557-2573.

Varughese, J.A., Menon, D. and Prasad, A.M. (2012), "Simplified procedure for displacement-based design of stepped buildings", *15th World Conf. on Earthq. Eng.*, Lisbon, September.

Varughese, J., A., Menon, D. and Prasad, M. (2015) "Displacement-based seismic design of open ground storey buildings", *Structural Engineering and Mechanics*, **54**(1), 19-33.

Vidot-Vega, A.L. and Kowalsky, M.J. (2013) "Drift, strain limits and ductility demands for RC moment frames designed with displacement-based and force-based design methods", *Engineering Structures,* **51**, 128-140.

Yang, B. and Lu, X. (2017) "Displacement-Based Seismic Design Approach for Prestressed Precast Concrete Shear Walls and its Application", *Journal of Earthquake Engineering.* https://doi.org/10.1080/13632469.2017.1309607

Zeris, C., Vamvatsikos, D., Giannitsas, P. and Alexandropoulos K. (2007), "Impact of FE modelling in the seismic performance prediction of existing RC buildings", *ECCOMAS Thematic Conference on Computational Methods in Structural Dynamics and Earthquake Engineering*, Rethimno, Greece.

Zhou, J., Zhao, W. and Mao, W. (2015) "Least Favorable Probability of Failure for 5-and 10-story RC Frame Structures with Vertical Irregularities," *Journal of Earthquake Engineering*, **19**(7), 1158-1180.

## Appendix

The following figures depict the section dimensions and detailing of the frames designed and analyzed herein.

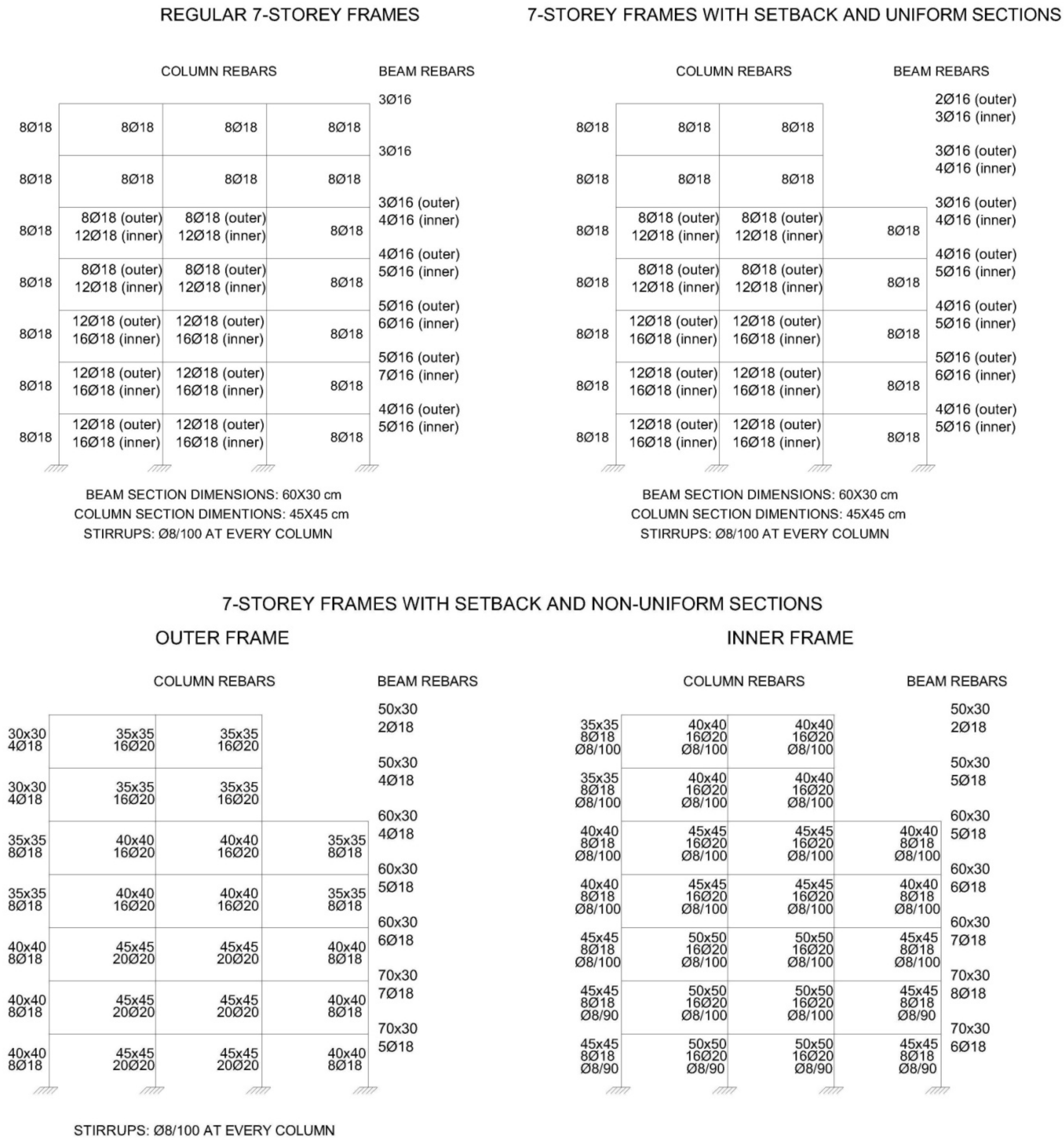


Fig. A1 Section dimensions and detailing of the Seven-Storey Frames R and A.

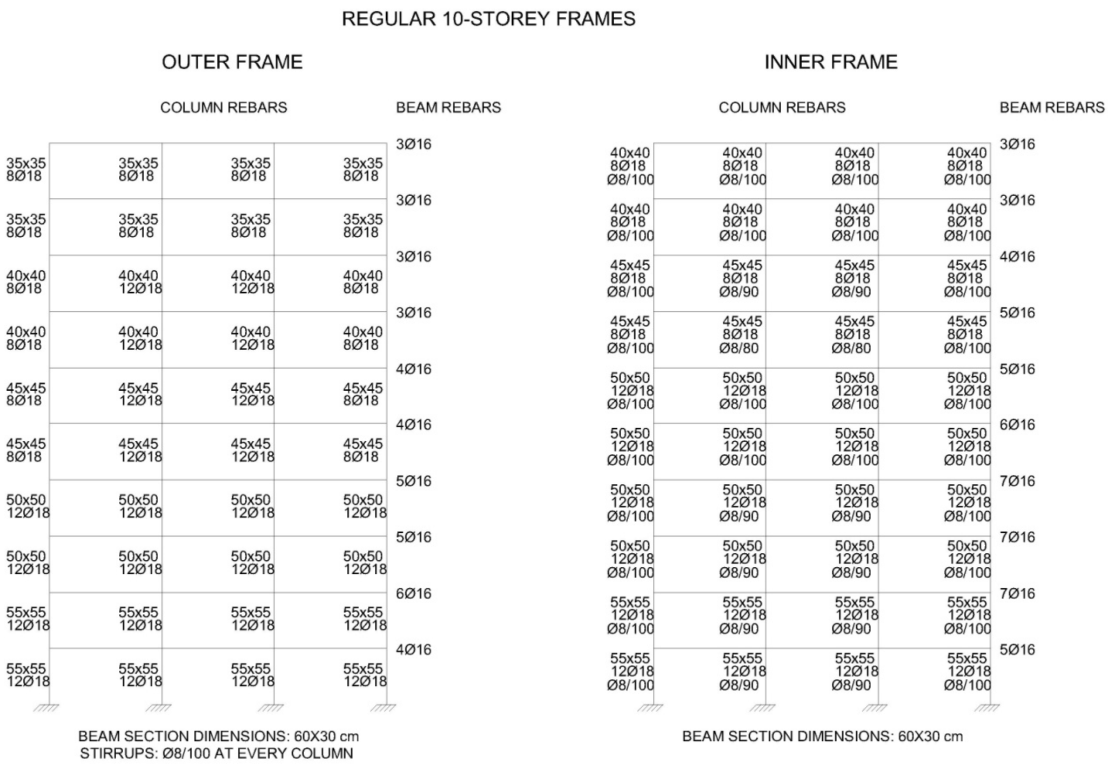


Fig. A2 Section dimensions and detailing of the Ten-Storey Frame R.

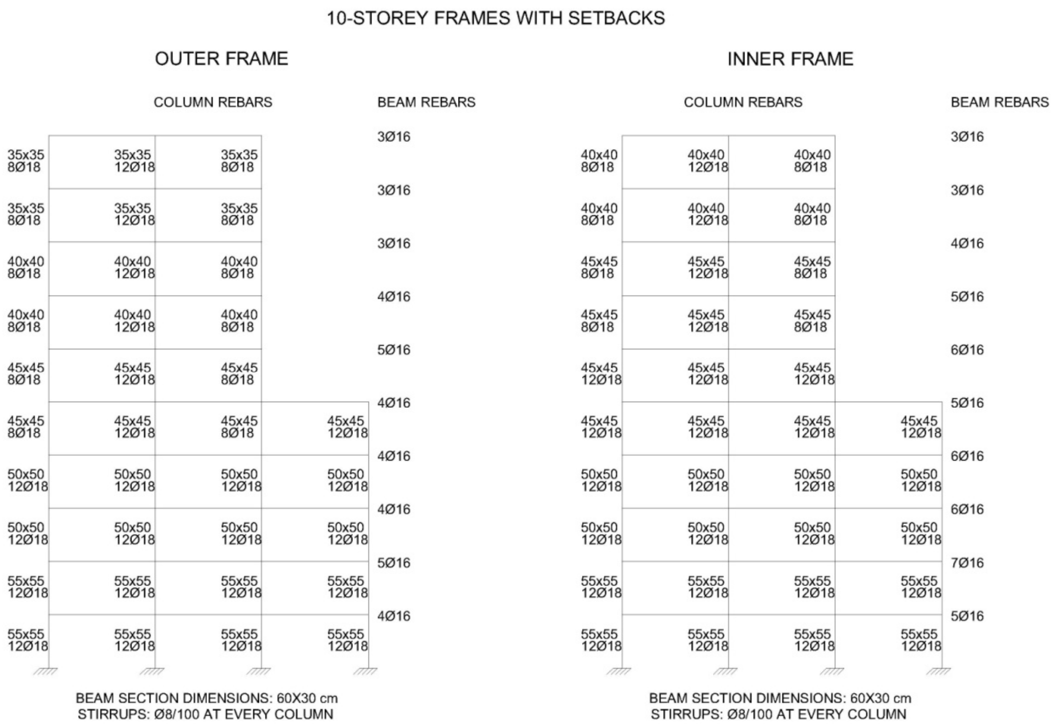


Fig. A3 Section dimensions and detailing of the Ten-Storey Frame A.

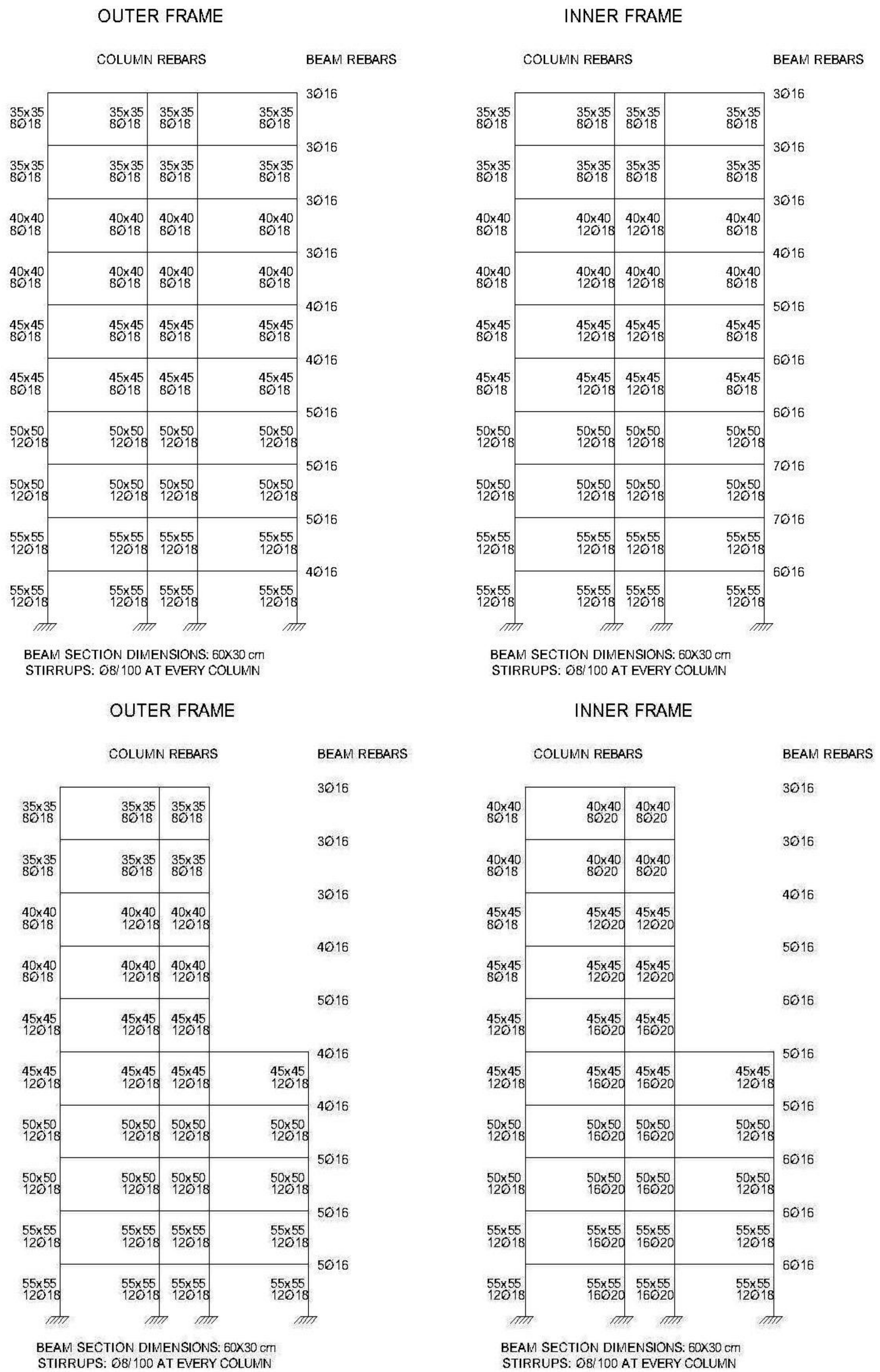


Fig. A5 Section dimensions and detailing of the Ten-Storey Frame B with Unequal Middle Bay length.

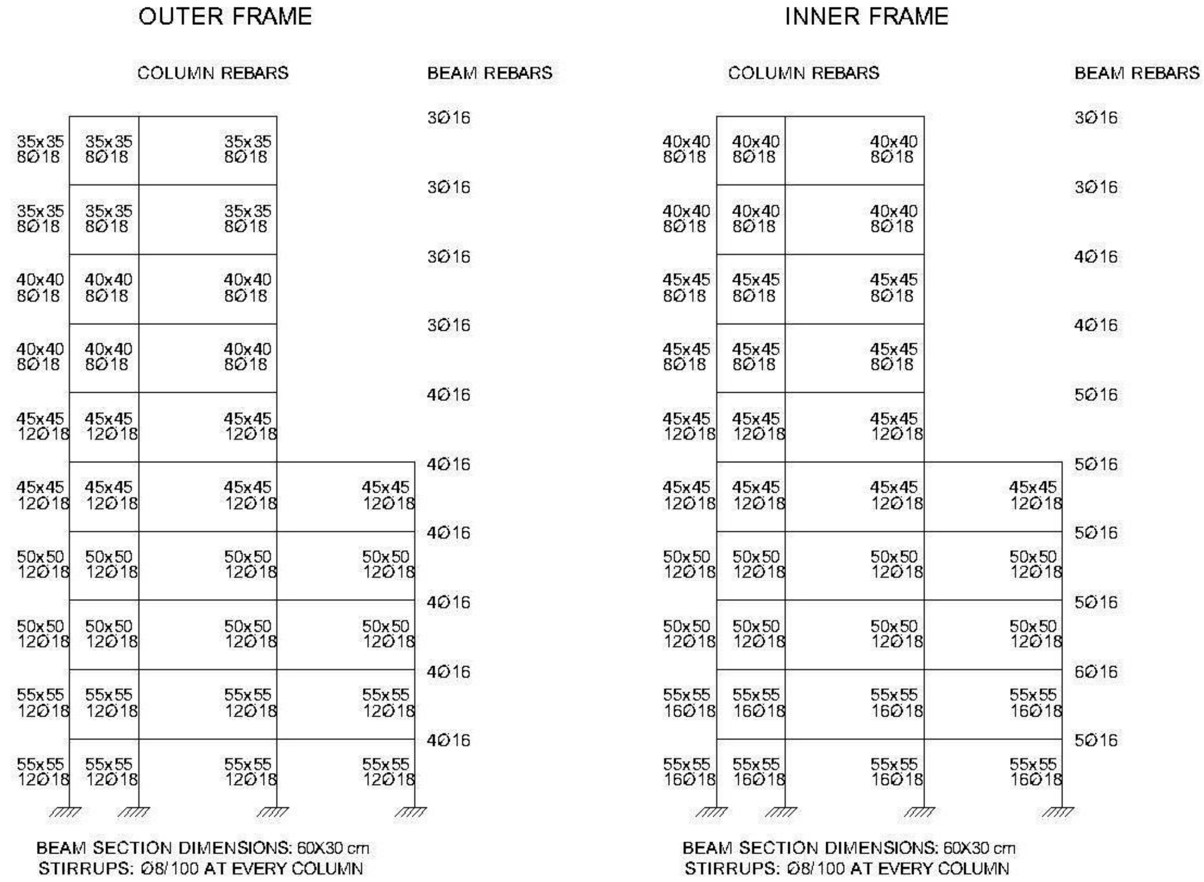


Fig. A6 Section dimensions and detailing of the Ten-Storey Setback Frame D with Unequal External Bay length.

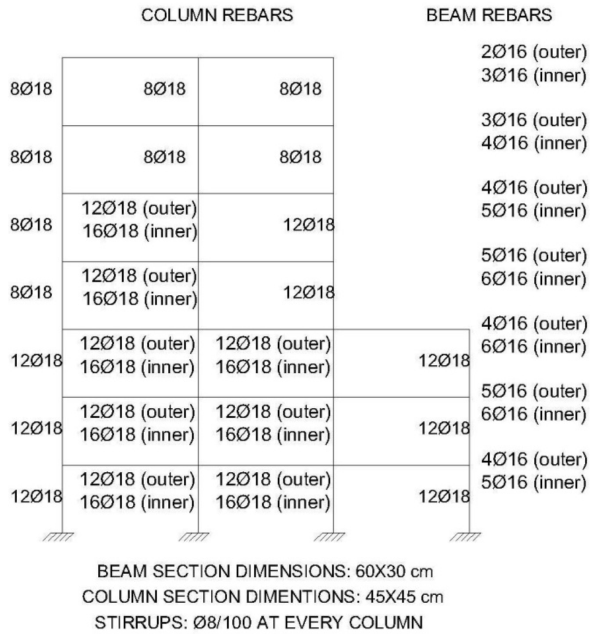


Fig. A7 Section dimensions and detailing of the Seven-Storey Tower Frame B.